Optimal Price Based Control of HVAC Systems in Multizone Office Buildings for Demand Response

U. Amin[1], M. J. Hossain[2], E. Fernandez [1]
[1]School of Engineering, Macquarie University, NSW 2109, Australia
[2]School of Engineering and Data Engineering, University of Technology Sydney, NSW 2007, Australia

Abstract

Optimizing the scheduling of heating, ventilation, and air-conditioning (HVAC) systems in multizone buildings is a challenging task, as occupants in various zones have different thermal preferences dependent on time-varying indoor and outdoor environmental conditions and price signals. Price-based demand response (PBDR) is a powerful technique that can be used to handle the aggregated peak demand, energy consumption, and cost by controlling HVAC thermostat settings based on time-varying price signals. This paper proposes an intelligent and new PBDR control strategy for multizone office buildings fed from renewable energy sources (RESs) and/or utility grid to optimize the HVAC operation considering the varying thermal preferences of occupants in various zones as a response of real-time pricing (RTP) signals. A detailed mathematical model of a commercial building is presented to evaluate the thermal response of a multizone office building to the operation of an HVAC system. The developed thermal model considers all architectural and geographical effects to provide an accurate calculation of the HVAC load demand for analyses. Further, Occupants' varying thermal preferences represented as a coefficient of a bidding price (chosen by the occupants) in response to price signals are modeled using an artificial neural network (ANN) and integrated into the optimal HVAC scheduling. Furthermore, a control mechanism is developed to determine the varying HVAC thermostat settings in various zones based on the ANN prediction model results. The effect of the proposed strategy on aggregator utility with wider implementation of the developed mechanism is also considered. The optimization problem for the proposed PBDR control strategy is formulated using a building's thermal model and an occupant's thermal preferences model, and simulation results are obtained using MATLAB/Simulink tool. The results indicate that the proposed strategy with realistic parameter settings shows a reduction in peak demand varying from 7.19% to 26.8%, contingent on the occupant's comfort preferences in the coefficient of the bidding price compared to conventional control. This shows that the proposed approach successfully optimizes the HVAC operation in a multizone office building while maintaining the preferred thermal conditions in various zones. Moreover, this technique can help in balancing the energy supply and demand due to the stochastic nature of RESs by cutting electricity consumption.

Keywords: Commercial buildings, demand response, energy imbalance, HVAC system, multi-objective optimization, real-time pricing.

Nomenclature

Variables

t, z	indices of time, zone
a , b	linear regression coefficients
t_1, t_2	Multizone office building working hours
n_1, n_2	Multizone office building working hours

Modeling Multizone Office Building HVAC Consumption

P_t^f	The total power consumed by the fan at time *t*
P_t^c	The total power consumed by the chiller at time *t*
P_t	Aggregated power usage of the HVAC System
q_t	The total load of the building
k_f	A parameter to consider the duct pressure losses and the fan efficiency
η	Chiller efficiency factor
COP	Chiller coefficient of performance
$m_z(t)$	Airflow rate in a zone at time *t*
$q_{z(t)}$	Zone load at time *t*
$T_{z(t)}$	Zone temperature at time *t*

T_s	Supply air temperature
$T_{o\,(t)}$	Outside air temperature
T_w	Chiller water temperature
$T_{z,sp}^t$	Modified temperature set-point at time *t*
$T_{z,ref(t)}$	Reference temperature of a zone at time *t*

Price Based Control Strategy

$P_{bc,z}^t$	Bidding price at time t in zone z
P_R^t	The retail price of electricity at time *t*
$P_{R(max)}^t$	The maximum value of electricity price at time *t*
$P_{R(min)}^t$	The minimum value of electricity price at time *t*
$T_{z,ref}$	Reference temperature of zone z
$T_{z,\max}$	Maximum temperature limit of zone z
$T_{z,\min}$	Minimum temperature limit of zone z
a_z^t	Temperature change rate at time *t* in zone z
ΔP^t	Retail and bidding price difference at time *t*
$\overline{\Delta P}^t$	Higher positive price difference at time *t*
$\underline{\Delta P^t}$	Lower positive price difference at time *t*
$-\Delta P^t$	Negative price difference
$\overline{U}_{t,z}$	Upper bound of price difference at time *t* in zone z
$\underline{U}_{t,z}$	Lower bound of price difference at time *t* in zone z
h_z	Number of price differences for zone z
ΔT^t	Temperature change at time *t*
$T_{z,sp}^t$	The thermostat new set-point temperature at time *t* in zone z
P_h^t	HVAC consumption at time *t*
$P_{th,z}^t$	Threshold price at time *t* in zone z

1. Introduction

1.1 Motivation

Commercial buildings' electricity consumption is about 26% of the aggregated consumption in Sydney, Australia. The commercial sector's contribution to the peak (26%) is higher than its contribution to total energy usage (19.3%) [1, 2]. The average annual growth in peak summer demand is approximately 3.8% a year, almost twice the rate of growth in total electricity consumption [3]. Heating, ventilation, and air-conditioning (HVAC) systems are responsible for nearly half (45%) of the commercial peak demand. Cooling, as the largest single load in Australia, accounts for more than 30% of the commercial peak demand [4]. Although the industrial sector dominates the total load demand, the joint commercial and residential HVAC operation are more dependent on temperature variations, while its contribution to the peak load increases from 17% to 20% over the peak hours on the hottest/most humid summer days [5]. The growing peak-hour demand puts considerable stress on power-supply companies to construct additional power plants and to maintain regulation services. However, much of this expanded capacity to accommodate the maximum possible peak demand lies idle other than for short periods. For instance, Australia's largest distributor of electricity has estimated that $11 billion in network infrastructure is used for the equivalent of four or five days a year [6]. Similarly, another distribution network has estimated that around 20% of network capacity is used for the equivalent of 23 hours per year [7]. Thus, to reduce the peak load of HVAC systems, TransGrid, Energy Australia and the New South Wales Planning Department jointly manage the Demand Management and Planning Project (DMPP). One of the activities of the DMPP is the widespread implementation of an innovative HVAC program that can reduce electrical demand during peak hours by replacing conventional HVAC systems with innovative HVAC technologies. The project team estimated the potential for a 300kVA reduction in peak demand at a cost of support of AU$242/kVA [5]. Although this program received an AU$1 million grant for implementation, the program failed due to timing and facilitation constraints.

Another approach to relieving the growing demand stress on the traditional power grid is to install renewable-based distributed generation at commercial buildings. However, the stochastic input from RESs can bring difficulty in balancing the electricity demand and supply [8]. Considering these challenges, an alternative way to reduce the peak demand/electricity consumption of HVAC systems is the control of HVAC thermostat settings in accordance with variations in electricity rates for demand response (DR) [9, 10]. The optimal scheduling of HVAC units has the potential to provide a low cost and grid reliable solution through the DR program. Motivated by the effectiveness of DR programs

to reduce electricity consumption and cost, this study proposed an easily implementable DR algorithm for a commercial building HVAC system.

1.2 Literature Review

The DR definition as provided in [11, 12] is "changes in electric usage by end-use customers from their normal consumption patterns in response to changes in the price of electricity over time, or to incentive payments designed to induce lower electricity use at times of high wholesale market prices or when system reliability is jeopardized". Based on this definition most of the DR programs are designed to alleviate the power system's burden during peak demand periods or emergencies. The utility incentivizes customers to modify, shift, and control their appliances consumption through DR programs [13]. As the highest percentage of electricity in a building is consumed by responsive/thermostatic loads such as air conditioners, refrigerators, and heaters [14], therefore, there are various benefits of controlling thermostatic loads including peak demand reduction, supply and demand balance to the microgrid with renewable sources, and voltage regulation, etc., [15]. The studies related to Price-based DR via control of HVAC thermostatic loads are mainly grouped into three main domains: Price-based DR control mechanisms, Price-based DR of HVAC systems with thermal comfort integration, and the modeling of HVAC systems for DR.

1.2.1 DR Control Mechanisms

The control of the thermostat for DR, in general, can be categorized as 1) transaction-based, and 2) price based. Transactive control (TC) utilizes a market-based control technology to make thermostatically controlled loads more demand responsive. The TC adjusts the thermostat setting based on the market-clearing price (MCP). However, in the price-based demand response (PBDR) program users change their energy usage pattern in response to changes in electricity pricing [10]. Time of use, real-time pricing (RTP) and critical peak pricing are different pricing mechanisms used for the DR program [16, 17]. Several designs of transactive controllers for residential as well as commercial building HVAC systems are available in the literature. For example, in [18, 19] Olympic Peninsula and American Electric Power projects investigate TC for residential HVAC systems. The researchers in [20] design the RTP in a transactive environment to define the final thermostat set-point of a residential HVAC based on the bidding price. In [21] similar design concepts are applied to those in [18, 19] to control the thermostat in commercial building HVAC systems. The work in [21] adjusted the zone temperature set-point based on the MCP. The adjusted set-point might be lower or higher than the desired set- point, so it might not strictly respect a customer's comfort preferences. Moreover, TC implementation required the extension of existing standards, and the development of new interface standards and many more studies are required to overcome the TC challenges [22, 23]. In contrast to [21], the current work proposes an easily implementable PBDR controller to change the thermostat setting by considering customer preferences in both thermal comfort and price selection.

1.2.2 Price-Based DR of HVAC Systems with Thermal Comfort Integration

In the literature, considerable work [24-30] has been done to design the Price-based DR algorithms for scheduling HVAC load in a single zone to obtain energy cost savings and/or energy efficiency. In [24] model predictive control system is developed to control HVAC units to reduce the peak power demand and electricity bills. The Co-optimization model for battery and HVAC scheduling is proposed in [25] to minimize power consumption during peak times. In [26] an advance control technique is presented for simultaneously minimizing the heating and cooling load of the HVAC systems for energy savings. However, these controllers do not consider a thermal comfort model for DR and are non-responsive to external price signals. In recent years, many research studies introduce HVAC load control strategies based on thermal comfort modeling and price signaling. For instance, in [28] a smart thermostat is developed where the desired comfortable levels set by consumers determine the on/off state of the air-conditioner; however, the smart thermostat is unable to respond to price signals. In [29], an economic model for the DR is presented which can calculate the shift in consumption pattern of individual consumers in response to TOU pricing. The work in [30] adopted the Stackelberg game to develop an incentive-based demand response scheme for residential HVAC load control in a small residential area including several houses. However, the proposed algorithms in [29, 30] neglect the issue of thermal comfort for consumers.

Recently DR strategies are proposed that respond to varying price signals while meeting user thermal comfort requirements. A hybrid price-based DR program is proposed in [31] to reduce the peak-to-valley index where the consumer's satisfaction is measured through the coefficient of variation percentage. In [32] a control algorithm is proposed that regulates the running state of HVAC units in a community microgrid according to the RTP with bounded temperature constraints for cost savings. In [33] and [34], controllers are designed using various mathematical approaches

to model a residential HVAC system. The developed controllers can reduce the peak consumption for HVAC of homes in response to RTP while taking into account thermal comfort requirements. In these strategies to consider the cost/comfort trade-off for consumers, when the energy price exceeds the maximum purchasing price of a customer, the thermostat setting will be increased by 2 to 3^{o}C, which may cause discomfort to many users. The mechanism designed in [35] and [36] controls the residential HVAC thermostat setting within a pre-determined thermal comfort interval in response to changing prices; in a single thermal zone. However, commercial buildings have multiple zones with a thermally interconnected dynamical system and therefore require careful attention to optimize the DR of HVAC systems. Considering this, unlike the above literature, the current work proposes a PBDR controller for a commercial building's HVAC operation, which involves a large number of occupants with varying thermal comfort preferences and with control of multiple zones.

Several studies highlighted the advantages for optimal utilization of the HVAC systems in multizone buildings for Price-based DR. A precooling strategy is considered in [37-39] to utilize commercial buildings' thermal storage potential for demand shifting during peak hours. In [40] a control strategy has been proposed for aggregation and coordination of industrial and commercial loads for DR using RTP. In [41] a predictive model of HVAC air-circulation fan power consumption is developed to use the commercial HVAC system for fast DR. Reference [42] investigates event-driven DR strategies to reduce commercial HVAC energy consumption. A commercial HVAC unit control method is presented in [43] for multiple-occupant spaces for optimal peak load reduction while maintaining human comfort using a predicted mean vote (PMV) model. In [44] fuzzy control is proposed to minimize the energy consumption of HVAC systems where the occupants' comfort is based on the acceptable range of the PMV index. In [45] control strategies are suggested to reduce the energy consumption of HVAC systems and maintaining the acceptable indoor air conditions related to thermal comfort. Likewise, in [46] a nonlinear model based on model predictive control is presented for the climate control of CO_2 concentration, temperature and relative humidity in a multizone HVAC system. However, these studies relied on a group level presentation of thermal comfort and were unable to reflect variations in behavior related to the thermal environment. The research studies [47, 48] show that at a certain temperature some occupants feel cooler and more uncomfortable than others due to differences in physiological and psychological responses based on gender and adaptive behavior. This implies that occupants have different thermal comfort preferences that need to be considered when designing an HVAC control strategy. Considering this, voting based participatory approaches were used in [49-51] to allow occupants to adjust their thermostat set-points according to their preference to integrate an individual occupant's preference into HVAC control. Moreover in [52], the thermal interaction between multiple zones is embedded in the controller design to analyze its effects on the HVAC control system. However, these strategies [43-50, 52, 53] are non-responsive to time-varying electricity prices for HVAC control. Though [51] considers the electricity pricing for HVAC control, it uses the ratio of weighted coefficients for occupants' thermal discomfort and the average price of electricity to trigger HVAC set-point temperature which is not suitable for high variations of electricity prices in the real-time market. Unlike these studies, in this paper, a practical and new dynamic PBDR control strategy is proposed to optimize the commercial building HVAC systems energy consumption, while considering the varying thermal comfort preferences of occupants in various zones in response to RTP signals.

1.2.3 Modeling of HVAC Systems for DR

To analyze the HVAC energy usage, the importance of accurate modeling of the HVAC system is undeniable. In the field of HVAC system modeling, the most complicated part is the development of an accurate model for a commercial building. This is because the components that need to be modeled for buildings are not limited to a building's construction. Internal building loads that include the number of people within the space, their activities and the heat gain from lighting must also be modeled [54]. The authors in [55] study the transmission of heat and moisture through the walls, roofs, and ceilings to estimate the indoor air temperature and humidity. However, they do not consider the transmission of heat and moisture through ventilation and internal loads. In [56] the research is focused on reducing the order of dynamic models of temperature and humidity in commercial multi-zone buildings for model-based HVAC control. References [57] and [56] use model predictive control that requires many assumptions to facilitate the HVAC energy usage calculations. The study in [58] and [59] only correlates the occupancy and air-infiltration rate with commercial building electricity consumption respectively. In this paper, a precise thermal and power model is developed for HVAC components by considering all the above-mentioned factors that influence the HVAC energy consumption.

1.3 Theoretical and Practical Contributions

This study is mainly motivated by the work in [51], but the developed price-based control strategy for a multizone office building in this paper is substantially different from this study. The main theoretical differences are:

- The published paper [51] considered individual preferences in a multizone building based on individual thermal discomfort levels. The control strategy in this paper inspired by well-known predicted mean vote (PMV) models in which the control of HVAC units in a multi-zone building depends on the group-level

presentation of thermal comfort [43, 60]. Different from these, individual thermal comfort preferences in each zone are taken into account [51] where the occupants' comfort is based on the acceptable range of the PMV index. In contrast to [51], the proposed strategy is a price-based demand response technique in where occupants can represent their thermal comfort preferences in terms of bidding price. Based on the retail electricity price forecast on a 30-minute basis, occupants in a multi-zone building bid the price they want to pay. Further, based on the retail and bidding price difference at time step t, the thermostat set-point in each zone is calculated.

- In [51] the minimum and maximum temperature limit determined by the standards for building space conditions, and temperature change rate in each zone (controlled by building operators) is constant and the same (1^{o}C). Unlike [51], in the proposed work, the controlled temperature limits in each zone varies within a specified building occupancy standards. Moreover, the temperature change rate in each zone varies from (0.25 to 1^{o}C) considering occupants' preferences. Further, the simulation result demonstrates that the HVAC consumption is minimum at low-temperature change rate compared to the high-temperature change rate by utilizing a developed control strategy. To the best of the author's knowledge, this is the first study that considered the temperature change rate effect on HVAC consumption and electricity bill savings in various zones considering various individual occupants' preferences in each zone such as bidding price, temperature limits and temperature change rate.
- In [51], the variable speed heat pumps were scheduled to operate with high power inputs during the hours when occupants' thermal discomfort level is high which results in high energy consumption. The occupant's thermal discomfort can be high in the hours when the peak demand occurs during the high price period, thus in this case, the developed strategy may not be able to cut peak electricity consumption if implemented by electric utility companies. Contrasting, numerical analysis demonstrates that the proposed strategy is effective to reduce the peak load and enable the utility providers to adopt effective demand management using real-time pricing.
- The work in [51] uses the ratio of weighted coefficients for occupants' thermal discomfort and the average price of electricity to trigger HVAC set-point temperature change in comparison to the current electricity price at time t. However, using this ratio as a trigger is not suitable for high variations of electricity prices in the real-time market. This may cause the controller not to increase the thermostat setting when the load should be curtailed. Unlike [51], the proposed controller uses the price difference between the current retail price and the dynamic bidding price that occupants change at each time step in various zones. This way the proposed strategy can control the HVAC thermostat setting considering fluctuations in electricity retail prices.

Compared with previous studies, the key practical contributions of this paper are:

- A commercial building HVAC system that is a complex, thermally interconnected dynamical system is considered, in contrast to residential buildings where researchers consider only one zone, which is cooled and heated up by the HVAC system. In this paper, five zones with varying thermal comfort preferences are controlled.
- Occupants' varying thermal preferences in the coefficient of the bidding price are modeled by employing an artificial neural network (ANN), which is trained using a machine-learning algorithm, and these preferences are directly integrated into the objective function in the optimal HVAC scheduling problem.
- A new PBDR control mechanism is proposed to control the HVAC thermostat setting in various zones to cater to the varying thermal preferences of occupants in response to RTP signals while maintaining the indoor environmental conditions of human occupancy in occupant-controlled multizone office buildings.
- Comprehensive simulation case studies are performed to show the effectiveness and applicability of the proposed PBDR controller.

1.4 Organization

The rest of the paper is planned as follows. Section 2 presents the HVAC system modeling, while Section 3 formulates the control problem and describes the pricing data. Section 4 presents the methods including proposed PBDR control strategy, prediction model and experimental set-up. Section 5 is devoted to the simulation results, while Section 6 provides a discussion on numerical results. Section 7 concludes the paper.

2 System Modeling

The structure of the proposed PBDR control methodology and a typical configuration of a commercial building HVAC system with multiple zones is shown in Fig. 1(a) and Fig. 1(b) respectively. The study considered multiple occupants in a multizone building getting power from RESs and/or power grid. Each zone is equipped with an HVAC controller, which has load control capabilities. The HVAC controllers are connected over a local area network (LAN) to a central control agent (CCA) that receives the occupant's comfort preferences in the coefficient of bidding price to control the thermostat setting in each zone. This study assumed that the CCA is owned, operated and maintained by the building manager. The main equipment of the HVAC system is air-handling units (AHU) and variable-air-volume (VAV) boxes responsible for producing and distributing cool/warm air for all zones. A detailed description of the air distribution system can be found in [61, 62]. The air moves through VAV boxes before reaching a given space, while the zone cool air mass flow rate delivered to space is controlled by changing the damper position at each VAV box. A thermal zone is a space that is cooled/heated by one VAV box. In this paper, a single centralized chiller is considered, which works for one AHU for providing cool/warm air to multiple zones, and a VAV box is associated with each temperature zone.

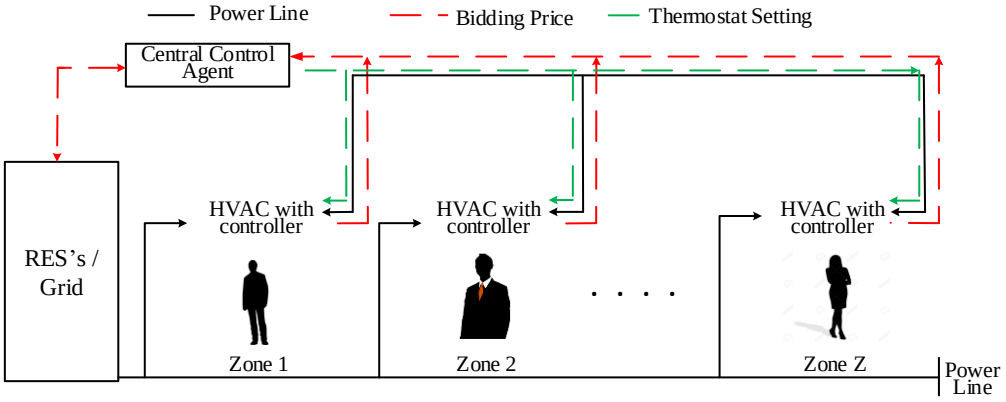

Fig. 1(a). System model depicting the flow of signals

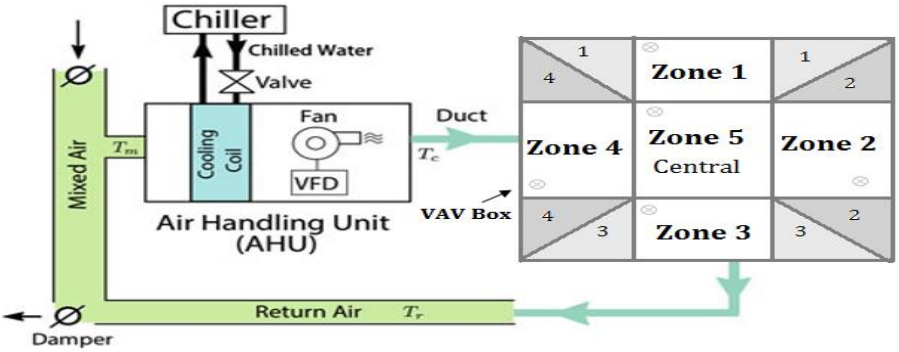

Fig. 1(b). Typical commercial building HVAC system configuration

2.1. Supply Fan Model

The fan power consumption principally depends on the air mass flow rate and the pressure difference between the inlet and outlet. Earlier simulation work [63] found that the AHU supply fan power versus fan mass flow rate fits a quadratic model. Also, the pressure drop is approximately linear with the total mass flow rate. With this form of fit and simplification, the fan power is modeled as a quadratic function of the total mass flow [64, 65]:

$$P_t^f = k_f(m(t))^2 \quad (1)$$

where P_t^f is the power consumed by the fan in kW to supply the required airflow rate to all zones, k_f (kW.s^2/kg^2) is the parameter that considers both the duct pressure losses and fan efficiency. The total supply airflow rate $m(t)$ is the sum of the airflow rate into each zone $m_z(t)$ in kg/sec and is given as

$$m(t) = \sum_{z=1}^{Z} m_z(t) \quad (2)$$

where z is the zone index, z= [1,…Z]. A zone airflow rate is dependent on the zone load, zone temperature, and supply air temperature. It can be expressed in mathematical form as [63]

$$\sum m_z(t) = \sum \frac{q_{z(t)}}{1.2(T_{z(t)} - T_s)} \quad (3)$$

where $q_{z(t)}$ is the zone load in kW, $T_{z(t)}$, T_s are the zone and supply air temperatures in °C, and 1.2 is a conversion factor.

2.2. Chiller Model

In the literature, comprehensive and complex chiller models are available [66, 67] but these models are not control-oriented. This paper considers a simple control-oriented chiller model [63, 65]:

$$P_t^c = \varphi \frac{\sum q_z(t)}{\eta COP} + (1-\varphi)\frac{q_t}{\eta COP} \quad (4)$$

where P_t^c is the total power consumed by the chiller in kW that is used to generate the chilled water consumed by the cooling coil for all zones, q_t is the total load of the building in kW, $\varphi \Rightarrow [0,1]$ is the damper position, η is the chiller efficiency factor and *COP* is the chiller coefficient of performance. q_t and *COP* can be calculated as

$$q_t = \sum m_z(t)\left(T_{o\,(t)} - T_s\right) \quad (5)$$

$$COP = 7.93\theta^3 - 21.12b\theta^2 + 16.49\,\theta + 2.22 + 0.1(T_w - 6) \quad (6)$$

where $T_{o\,(t)}$, T_w are the outside air and chilled water temperatures in °C, and θ is the cooling coil and design load ratio.

2.3. HVAC Power Consumption

The aggregated power usage of the HVAC system is the sum of the fan and chiller power consumptions as given

$$P_t = P_t^f + P_t^c \quad (7)$$

Putting the values of (2), (3) into (1), and (5) into (4), (7) over the given time horizon for Z zones can be re-written as:

$$P_t = \sum_t^w \sum_z^Z \{(k_f * \left(\frac{q_{z(t)}}{1.2(T_{z(t)} - T_s)}\right)^2) + (\varphi \frac{q_{z(t)}}{COP} + (1-\varphi)\frac{m_{z(t)}(T_{o\,(t)} - T_s)}{COP}) \quad (8)$$

where P_t is the total power consumed by the HVAC load in kW and *t* is the time index, *t* = [1….W]. It can be noted from (8) that the fan and chiller power consumptions depend on the zone load. Therefore, to provide reliable and accurate DR, a precise calculation of the zone load is required.

2.4. Zone Cooling and Heating Load

The key design component for most HVAC systems is an accurate assessment of the cooling load (CL) and heating load (HL) requirements because these loads can significantly affect the comfort and the productivity of the occupants, the operating cost and the energy consumption [68]. The peak HL in winter months occurs before sunrise and there is no considerable change in the outside environment during the winter season. In contrast, in summer, solar radiation causes a significant variation in outdoor environmental conditions throughout the day, and all indoor heating components add to the CL. Therefore, CL calculations are fundamentally more complex and require consideration of unsteady-state processes [69]. Moreover, the CL's contribution to the commercial peak load is the largest [4]. For these reasons, this paper considers zones with cooling requirements only and presents detailed mathematical modeling of the CL calculation based on the cooling load temperature difference (CLTD) method with solar CL factors suggested by the American Society of Heating, Refrigeration and Air-Conditioning Engineers (ASHRAE). This method considers all factors that influence the HVAC electricity consumption such as building size, outdoor environmental conditions, indoor activities, and thermal load, etc.

2.5. Cooling Load Calculation

The building CL is the sum of the external and internal CL of each zone $q_c^z(t)$ and it includes both sensible and latent CL components [69]. The sensible load refers to the dry-bulb temperature, while the latent load refers to the wet-bulb temperature of the zone [70]. The CL heat balance model is based on dynamic conditions, which consider the heat stored in the building envelope and interior materials.

2.5.1 External Cooling Load Calculation

The heat transferred through the building's roof, walls and glass is called the external CL [69]. The basic conduction equations for heat gain/conductive load from roof, wall, and glass are given as

$$q_r(t) = \cup_r * A_r * CLTD_r^c \text{ (t)} \quad (9)$$

$$q_w(t) = \cup_w * A_w * CLTD_w^c \text{ (t)} \quad (10)$$

$$q_g^c(t) = \cup_g * A_g * CLTD_g^c \text{ (t)} \quad (11)$$

The solar load through glass is the sum of a conductive and a solar transmission load that occurs when solar radiation is absorbed, stored and scattered in the atmosphere. The solar transmission load through glass is given as
The sum of the CL through glass can be calculated as

$$q_g^s = A_g * S_c * S_{cl} \quad (12)$$

$$q_g(t) = q_g^c(t) + q_g^s \text{ (t)} \quad (13)$$

where $q_r(t)$, $q_w(t)$, $q_g(t)$ are the hourly heat gains by conduction through roof, wall, and glass in watts, $\cup_r$, $\cup_w$, $\cup_g$ are the thermal transmittances for roof, wall, and glass in W/m^2.C, A_r, A_w, A_g are the areas of roof, wall, and glass in m^2, $CLTD_r^c\ (t)$, $CLTD_w^c\ (t)$, $CLTD_g^c\ (t)$, are the hourly-corrected CLTD values for roof, wall, and glass in ^{o}C, S_c is the shading coefficient, S_{cl} is the solar CL factor, $q_g^c(t)$, q_g^s (t) are the conductive and solar transmission components of the glass load in watts. In [70] hourly CLTD values for roof ($CLTD_r$), wall ($CLTD_w$) and glass ($CLTD_g$) are provided for one typical set of conditions. Therefore, it is required to calculate the CLTD correction factors for roof, wall, and glass according to Sydney weather conditions. The CLTD correction factors can be calculated as:

$$CLTD_r^c = [CLTD_r + (T_{in}^D - T_{in}^R) + ((T_o^{DB} - DR/2) - T_o^M)] \quad (14)$$

$$CLTD_w^c = [CLTD_w + (T_{in}^D - T_{in}^R) + (T_o^{DB} - DR/2) - T_o^M)] \quad (15)$$

$$CLTD_g^c = [CLTD_g + (T_{in}^D - T_{in}^R) + (T_o^{DB} - DR/2) - T_o^M)] \quad (16)$$

where T_{in}^D, T_{in}^R are the indoor design and indoor room temperatures, T_o^{DB}, T_o^M are the outdoor dry bulb and mean daily temperatures and DR is the daily temperature range in ^{o}C. Climatic design conditions for Sydney are taken from [68] and these are based on long-term (20-25 years) hourly observations.

2.5.2 Internal Cooling Load Calculation

The heat generated by occupants, equipment, and lights in a zone is called the internal load [69]. The various internal loads (e.g. occupants and appliances) consist of sensible and latent heat transfers, but the lighting load is sensible. The conversion of the sensible heat gain to space CL is affected by the thermal storage characteristics of that space. However, the latent heat gains are considered to be instantaneous [68].

2.5.2.1 Heat Gain from People and Appliances

The CL due to occupancy and appliances is the sum of sensible and latent CL components [69]. The sensible and latent CL from people and appliances is calculated as:

$$q_p^s(t) = N * q_h^s * CLF_p \quad (17)$$

$$q_p^{lt} = N * q_h^l \quad (18)$$

$$q_a^s(t) = q_a^{in} * U_f * R_f * CLF_a \quad (19)$$

$$q_a^{lt} = q_a^{in} * \cup_f \quad (20)$$

(17) and (18) are used to calculate the dynamic occupancy patterns in a zone. The total CL due to occupancy and appliances is given as:

$$q_p(t) = q_p^s + q_p^{lt} \quad (21)$$

$$q_a(t) = q_a^s + q_a^{lt} \quad (22)$$

where N is the number of people in a zone, q_h^s, q_h^l are the sensible and latent heat gains due to individuals' activities in watts, CLF_p, CLF_a are the people and appliances CL factors by an hour of occupancy, q_a^{in} is the rated energy input from appliances in watts, U_f, R_f are the usage and radiation factors of appliances, q_p^s, q_p^{lt}, q_a^s q_a^{lt} are the sensible and latent cooling loads (CLs) from people and appliances in watts. CLF_p, CLF_a capture the time lags of the CLs affected by the building's thermal mass.

2.5.2.2 Lighting Heat Transfer

The sensible CL from lighting is given by

$$q_l = W * L_{uf} + SB_{af} * CLF_l \quad (23)$$

where W is the lighting load in watts, L_{uf} is the lighting use factor, SB_{af} is the special ballast allowance factor and CLF_l is the CL factor of light, by an hour of occupancy.

2.5.2.3 Heat Transfer through Infiltration Air

The infiltration air CL has both sensible and latent load components and can be calculated as

$$q_{ia}^s(t) = A_f(t) * (T_{o,t} - T_{i,t}) \quad (24)$$

$$q_{ia}^{lt}(t) = A_f(t) * (W_{o,t} - W_{i,t}) \quad (25)$$

The total infiltration air CL is given by

$$q_{ia}(t) = A_f(t) * (h_{o,t} - h_{i,t}) \quad (26)$$

where $A_f(t)$ is the infiltration airflow rate in m^3/min, T_o, T_i ^{o}C, W_o, W_i gm/gm, h_o, h_i J/gm are the outside and inside dry bulb temperatures, humidity ratio, and air enthalpy respectively, q_a^s, q_{ia}^{lt} are the sensible and latent CL in watts due to infiltration air. The values of the shading coefficient, solar CL, lighting, and people CL factors, and the rates of sensible and latent heat gain from occupancy are taken from [70].

2.5.3 Zone Load Calculation

The zone CL is the sum of all external and internal CL components and is given by

$$q_z(t) = [q_r(t) + q_w(t) + q_g(t) + q_p(t) + q_a(t) + q_l(t) + q_{ia}(t)] \quad (27)$$

where $q_r(t), q_w(t), q_g(t)$ are the total CLs for roof, wall, and glass, $q_p(t),\ q_a(t),\ q_l(t),\ q_{ia}(t)$ are the total CLs due to occupancy, appliances, lights and infiltration air, q_z is the aggregate CL of the zth zone in kW.

]

3. Control Problem and Pricing Data

In this section, a general control problem is formulated using the model developed in Section 2, and detail about pricing information is given.

3.1 Problem Formulation

The proposed model has two objectives: (1) minimizing the peak load demand and the aggregated power usage (P_t) of the HVAC system, and (2) minimizing the difference between the controllable/modified temperature set-point and the desired reference temperature of the zone. The objective function of the proposed model can be is re-written as:

$$min_{q_z[.],T_{z,ref}[.]} = \sum_t^W \sum_z^Z \{(k_f * \left(m_z(t)\right)^2) + \ (\varphi \frac{q_{z(t)}}{COP} + (1-\varphi)\frac{q_t}{COP})\}[53][53][\quad (28)$$

$$+ \sum_t^W \sum_z^Z \left(T_{z,sp}^t - T_{z,ref(t)}\right)$$

subject to the following constraints due to control requirements:

$$m_{z,min} \le m_z(t) \le m_{z,max} \quad (i)$$

$$T_{z,sp}^t, T_{z,ref(t)} \in \left[T_{z,max}, T_{z,min}\right] \quad (ii)$$

$$q_{z,min} \le \frac{q_t}{1.2\ (T_{z(t)} - T_s)} \le q_{z,max} \quad \forall\ t \in [1 \ldots W] \quad (iii)$$

where $m_{z,min}, m_{z,max}, q_{z,min}, q_{z,max}$ and $T_{z,min}, T_{z,max}$ are lower and upper bounds of the zth zone's, supply airflow rate, zone load, and zone temperature respectively. In (28) $T_{z,sp}^t$, $T_{z,ref(t)}$ represent the modified temperature set-point to save energy and the reference temperature of a zone at time *t*. The first term in the objective function computes the aggregated HVAC energy consumption over W time intervals. The energy consumption is a function of the cooling load $q_z(t)$ as defined in (8), usually in kW per hour. Since the time interval is assumed to be 30 minutes in this study, the hourly usage on a 30 min basis is divided by 2 in the objective function. The temperature deviations between modified thermostat set-points and the reference temperature set-point in a zone are handled by the second term in the objective function. The controller aims to keep the modified/inside temperature close to a reference temperature set-point by minimizing the deviation between the two in various zones. In conventional control, commercial HVAC units' operation is based on a reference temperature set-point that does not change frequently throughout the considered period, and thus the HVAC operates regardless of price fluctuations. The reference temperature is chosen by a building manager/aggregator taking into account a group level presentation of thermal comfort in a multizone office building. The major drawback of conventional control is that with a fixed reference temperature set-point both the aggregator and consumers are unable to utilize the advantages of dynamic electricity pricing, while the above model overcomes this drawback by operating the HVAC unit at variable thermostat set-points in response to the price fluctuations in various zones. The deployment of variable thermostat settings in various zones achieves financial benefits while keeping the indoor environment within the occupants' thermal comfort limit. Therefore, the current work proposes a DR strategy for determining cost-efficient variable thermostat set-points for a PBDR controller within a temperature range specified in constraint (*ii*). The variable thermostat settings in various zones are determined as a function of the occupants' chosen bidding price at each time *t* as a response to price fluctuations. The proposed PBDR control strategy is discussed in Section 4.

3.2 Pricing Data

Pricing data is obtained from the Australian Energy Market Operator (AEMO). Wholesale electricity prices are decided by AEMO depending on the supply and demand at a 5-minute interval and the average over every 30 minutes. On the AEMO website, the day-ahead wholesale electricity priced on a 5-minute and 30-minute basis is available. The pricing system in Australia adopts an RTP structure in the wholesale market and a TOU tariff in the retail market for customers with smart meters. However, TOU tariffs do not reflect the actual variations of the wholesale price at the time of consumption. To coin the real-time wholesale price structure for the retail market the authors in [71] design the real-time retail price. They have shown that the retail price follows the pattern of the wholesale price. Based on this, the half-hour ahead forecasts wholesale energy settlement price is considered as the real-time retail price of electricity in this paper. Half-hour ahead electricity prices are chosen because Australia's National Electricity Market operates as a continuous-trading market for each half-hour interval [72]. Moreover, the retail electricity price on a 30-minute basis is preferred over 5-minute and hourly-based pricing for the following reasons. Significant accessible computing resources and software would be required to implement 5-minute settlement intervals. New spike loads away from the expected peak hours occur when hourly pricing is implemented, therefore this new aggregated load affects the utility. The effective spread of demand after the typical peak occurs with 30-minute based retail prices of electricity [73]. Fig. 2 shows the 30-

minute based day-ahead time-varying electricity price obtained from the AEMO electricity market [74]. The chosen electricity price is on a typical hot summer day of 6 November 2018. The electricity value on that particular day is chosen carefully considering historical electricity prices. It represents those hot summer days where the peak electricity price substantially increases from the average price of electricity.

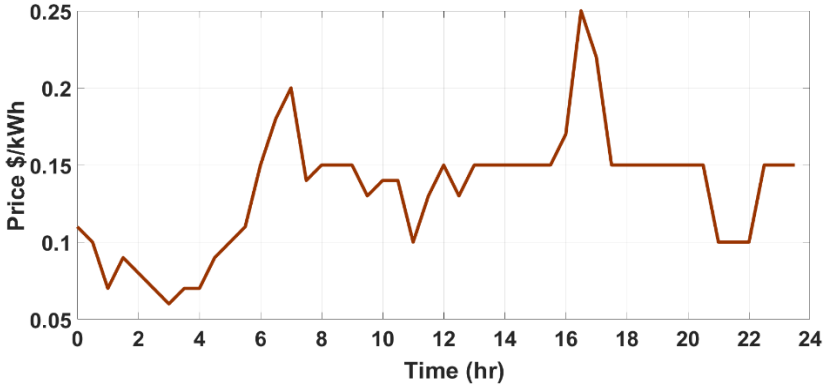

Fig. 2. Day-ahead retail electricity price on a hot summer day

4. Methods

4.1 Price-Based Demand Response Control Strategy

The proposed price-based demand response (PBDR) controller is responsible for controlling the thermostat setting in z ϵ Z zones in a multizone office building. It is assumed that each zone has multiple rooms with a number of occupants as shown in Fig. 1(a) and they have varying thermal comfort requirements in each zone. In this study, occupants in Z zones reflect their thermal preferences in a coefficient of bidding price ($P_{bc,z}^t$). This is a price of electricity that occupants of various zones offer considering variations in retail price (P_R^t) at each 30-minutes timestamp *t*. Occupants in Z zones can select a reference temperature ($T_{z,ref}$), minimum ($T_{z,\min}$) and maximum temperature ($T_{z,\max}$) and set-point interval (a_z^t) to further express their thermal comfort preferences. $T_{z,ref}$ is the desired temperature at which most of the occupants in a zone feel comfortable, and that may be the same or different in each zone. $T_{z,\min}$and $T_{z,\max}$ represent the allowable temperature range in response to the variation of P_R^t. If the occupants of a certain zone feel cooler at time *t*, they bid considerably lower than the retail price, which indicates that the occupants want to increase the thermostat set-point from the reference temperature. In contrast, a bidding price higher than the retail price reflects the feeling of warmth, and thus a decrease in the thermostat set-point is required from the reference temperature. Meanwhile, a bidding price equal to the retail price signifies that the occupants want to maintain the thermostat at the reference temperature set-point.

The proposed PBDR controller calculates the price difference (ΔP^t) between P_R^t and $P_{bc,z}^t$ in Z zones on a 30-minute basis for a total simulation time $t \in W$. The controller will take control action when P_R^t is higher or lower than $P_{cb,z}^t$ by increasing or decreasing the temperature in each zone based on the price difference (ΔP^t). If P_R^t is equal to $P_{cb,z}^t$, the thermostat from the PBDR controller maintains the $T_{z,ref}$ set by the occupants in a zone. The controller changes the set-point of the thermostat within a range of $T_{z,min}$ to $T_{z,\max}$ in a zone in response to P_R^t. When $P_{bc,z}^t$ is significantly lower than P_R^t at time step *t* then the thermostat can be set to $T_{z,\min}$and when it is substantially higher than P_R^t then the thermostat setting can be as high as $T_{z,\max}$. The temperature change (ΔT^t) from the previous setting at each time depends on the set-point interval a_z^t. Previous controllers [28, 32][20] either compare the current retail price with the last day's average price of electricity or a constant threshold price to change the thermostat setting. However, using an average price or a constant threshold price is not suitable for high fluctuations in the retail price in the real-time market. This may cause the controller to not increase the thermostat setting when the load should be curtailed. Moreover, a constant threshold price is unable to consider the varying thermal comfort preferences of occupants in a multizone office building. In contrast, the current work compares the retail price with the dynamic bidding price $P_{cb,z}^t$ that occupants change at each time step in various zones. This way the proposed strategy can cater to the occupants' varying choice of $P_{bc,z}^t$ with respect to time-varying P_R^t. Furthermore, in previous studies [27, 28, 57], the coefficient for comfort is unitless and thus it is difficult for occupants to show their comfort preferences in response to price signals, while the proposed strategy allows them to choose the comfort coefficient of their preference.

Occupants in a multizone building will choose $P_{cb,z}^t$ at each time step to change the thermostat setting according to their requirements. The feasible range of $P_{cb,z}^t$ is given as

$$P_{R(min)}^t \leq P_{cq,z}^t \leq P_{R(max)}^t \quad (29)$$

where $P^t_{R(min)}$, $P^t_{R(max)}$ are the minimum and maximum values of the 30-minute ahead forecast retail electricity price. Equation (29) implies that $P^t_{cb,z}$ should be greater than the minimum value of the 30-minute ahead forecast retail electricity price $P^t_{R(min)}$, and it can be as high as the maximum value of the retail price $P^t_{R(max)}$ according to customers' comfort preference at time *t*. According to (29) occupants cannot bid less than $P^t_{R(min)}$to participate in the DR program.

Since the occupants' choice of bidding price at each time step *t* in a zone follows the variations of P^t_R which corresponds to their thermal comfort preferences obtained by the desired thermal comfort is evaluated based on the price difference between P^t_R and $P^t_{cq,z}$. The price difference ΔP^t is the subtraction of the electricity retail price P^t_R from the bidding price $P^t_{cq,z}$ and it is calculated at each timestamp *t* in various zones when the new retail price is updated in every 30 minutes as

$$\Delta P^t = P^t_R - P^t_{cq,z} \tag{30}$$

When P^t_R is higher (lower) than $P^t_{cq,z}$, ΔP^t are a positive (negative) number and the PBDR controller starts to work. Otherwise, ΔP^t is zero and the controller stops working immediately and maintains or returns to $T_{z,ref}$.

The magnitude of the price difference is used to evaluate the different occupants' thermal comfort preferences, and based on this they are categorized into three main types:

1) high comfort; 2) moderate comfort; 3) low comfort

High comfort occupants' bidding price $P^t_{cb,z}$ is equal/close to P^t_R for most of the occupied hours, which leads to a zero /lower positive price difference ($\underline{\Delta P}^t$). Thus, a zero/ low magnitude of the positive price difference $\underline{\Delta P}^t$ indicates higher requirements on thermal comfort and consequently, the designed strategy maintains the thermostat at the reference temperature/allows temperature variations close to the reference temperature set-point respectively. For other hours, the bidding price $P^t_{cb,z}$ can be higher than P^t_R , which results in a negative price difference ($-\Delta P^t$) and thus thermostat set-point is decreased from the reference temperature.

In contrast, low comfort occupants' bidding price $P^t_{cb,z}$ is significantly lower than P^t_R for most of the occupied hours, which results in a higher positive price difference ($\overline{\Delta P}^t$). The high magnitude of the positive price difference $\overline{\Delta P}^t$ represents a lower thermal comfort requirement (and hence a higher temperature set-point). For the remaining hours, the bidding price can be equal/close to P^t_R to maintain the thermostat at/near the reference temperature set-point. Meanwhile, modest comfort occupants' bidding prices reasonably vary from P^t_R for most of the occupied hours for a moderate temperature variation from the reference temperature set-point. Moreover, in a high/moderate comfort zone $T_{z,max}$ is lower than for a low comfort zone and this suggests that, in these zones at times of high retail price, the maximum temperature variation is lower than the low comfort zone.

The magnitude of the price difference can be negative, zero and low at times of a low retail price in various zones, however, it increases correspondingly in each zone as the retail price increases and yields a higher positive price difference $\overline{\Delta P}^t$. The upper and lower bound of the price difference in each zone is different and can be calculated using (31) and (32) respectively.

$$\overline{U}_{t,z} = P^t_{R(max)} - P^t_{cq,z(max)} > 0 \tag{31}$$

$$\underline{U}_{t,z} = P^t_R - P^t_{cq,z} \leq 0 \tag{32}$$

where $\overline{U}_{t,z}$, $\underline{U}_{t,z}$ are upper and lower bounds of the price difference and $P^t_{R(max)}$, $P^t_{cq,z(max)}$ are the maximum values of the retail and bidding prices in a zone during occupancy hours. Equation (31) implies that, at a time of maximum retail price, the occupants bid the maximum price $P^t_{cq,z(max)}$ so that the temperature variation does not exceed the maximum temperature limit $T_{z,max}$ set by the occupants in a zone. This suggests that at the upper bound of the price difference $\overline{U}_{t,z}$, the thermostat is set at $T_{z,max}$ in a zone. Since a high comfort occupant's maximum temperature limit $T_{z,max}$ is lower than for low comfort occupants, they bid considerably higher than other occupants at times of maximum retail price, and thus the value of the upper bound $\overline{U}_{t,z}$ is lower in the high comfort zone than in the low comfort zone.

The lower bound of the price difference $\underline{U}_{t,z}$ represents the minimum price difference between the retail and bidding prices at time step *t* when the retail price is low. The value of the lower bound $\underline{U}_{t,z}$ can be negative or zero in high and moderate comfort zones but it is zero in low comfort zones to approach the minimum temperature limit $T_{z,min}$ that is less than/equal to the reference temperature $T_{z,ref}$ in high and moderate comfort zones but equal to $T_{z,ref}$ in low comfort zones.

4.2 ANN-based Prediction Model

Since the control action of the PBDR strategy is based on the price difference ΔP^t to change the set-point temperature, it is required to calculate the thermostat setting as a function of ΔP^t. To model the relation between the changes in price with the temperature a prediction model with an ANN is used. Initially, the bidding is carried out and the market is cleared at the agreed price. This clearing value is one of the parameters used to predict the change in temperature with the bidding price. The inputs to the ANN are the outside temperature, preferred indoor temperature, the bidding price, retail price, and the agreed price. The output of the network is a relation between the bidding price, retail price, and indoor temperature. Therefore, for n days the number of inputs to the ANN function is 5 × n × 24, which represents the inputs to the training algorithm, and the output is a 1 × n × 24 matrix as shown in Fig. 3. The model was trained with 20 hidden layers and the mean square error (MSE) was the stopping condition. The training was performed with data for a year, with a resolution

of 1 hour, i.e. the data set had a length of 8760. The neural-network model accurately reflected the relationship between the bidding price, retail price and the thermal behavior of the user at the given weather profiles. Fig. 4 shows the training, validation and test phases of the machine-learning algorithm, which indicates that the training produces a good fit.

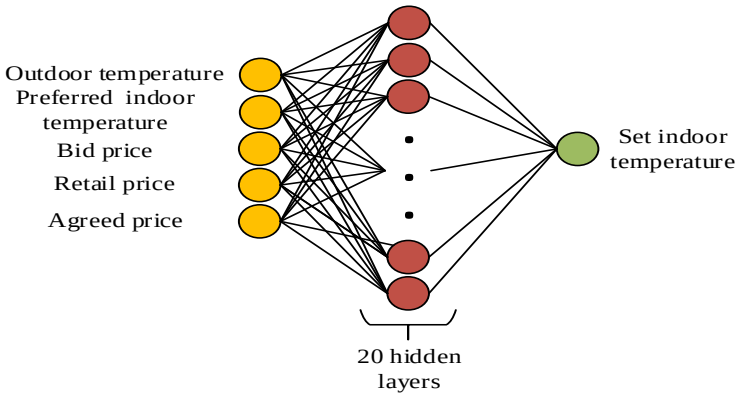

Fig. 3. The neural network training model

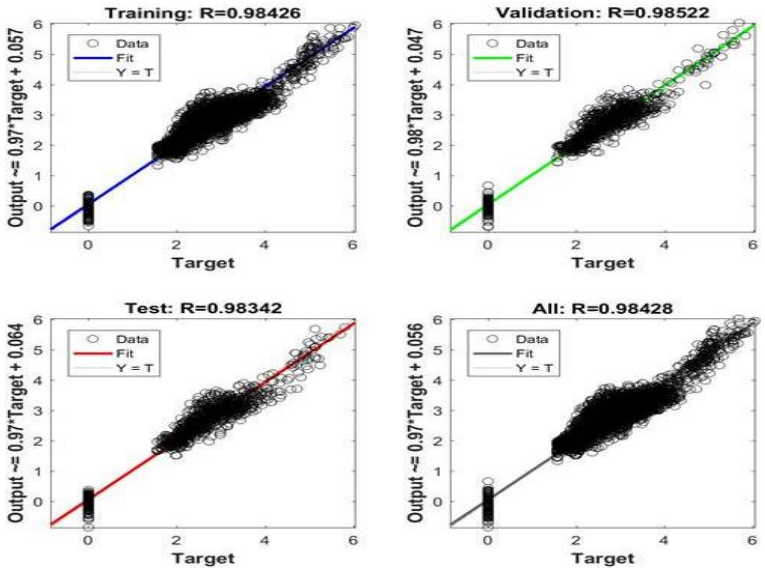

Fig. 4. Prediction model results based on artificial neural network

A linear regression model is used to represent the ANN prediction model, resulting in the mathematical form

$$\Delta T^t = a\,\Delta P^t + b \tag{33}$$

where a and b are linear regression coefficients. Equation (33) converts the price difference ΔP^t to the temperature change ΔT^t that the thermostat accepts. The ANN prediction model results in the form of (33), implying that 1 ΔP^t, which is equivalent to 0.01 AU$/kWh, results in an increment of 0.25 ºC in the thermostat setting to decrease the HVAC load. In other words, four times the price difference ($4\Delta P^t$) is used to increase the thermostat setting by 1ºC for energy saving at peak hours. In previous work, when the retail price is much higher than the threshold price, the temperature sharply increases by 2 to 3ºC. The sharp rise in temperature is undesirable for the following reasons: 1) it may affect human health through thermal shock; 2) it gives a large mechanical burden to the heat pump; 3) some customers feel discomfort in a high-temperature difference from the initial set-point when the retail price is higher for an extended period. In this paper, considering these drawbacks and the varying thermal preferences of occupants, the temperature change is discretized to a set-point interval a_z^t, which varies from 0.25 to 1ºC maximum according to the occupants' choice at each time t. Further the number of price differences (h_z) in each zone for a given time is given by (34) and depends on the temperature range and occupants' chosen set-point interval a_z^t.

$$h_z = \frac{T_{z,max} - T_{z,ref}}{a_z^t} + 1 \quad (34)$$

The number of price differences h_z is negatively correlated with the set-point interval, being higher in a low set-point interval zone and decreasing with a high set-point interval. This is because with a low set-point interval there are more temperature variations within an occupants' chosen temperature range $[T_{z,max} - T_{z,min}]$ in a zone.

The new set-point temperature T_{sp}^t with a temperature change ΔT^t from the reference temperature at a bidding price $P_{cb,z}^t$ higher, lower or equal to the retail price P_R^t is determined as

$$T_{z,sp}^t\ [C^o] = \begin{cases} T_{z,ref} + \Delta T^t & if\ \ P_R^t > P_{cb,z}^t = +\Delta P^t \quad (35.a) \\ T_{z,ref} - \Delta T^t & if\ \ P_R^t < P_{cb,z}^t = -\Delta P^t \quad (35.b) \\ T_{z,ref} & if\ \ P_R^t = P_{cb,z}^t = 0\ \Delta P^t \quad (35.c) \end{cases}$$

The above equations calculate the new set-point temperature for the thermostat settings according to the temperature change ΔT^t that depends on the price difference ΔP^t. The thermostat set-points are calculated in advance using a 24-hrs ahead forecast half-hourly RTP signal. Equation (35.a) operates the HVAC system at a higher temperature than the reference temperature when the electricity retail price is higher, and consequently, the HVAC consumption is reduced. Equation (35.b) ensures that the HVAC is set to a lower set-point than the reference temperature to make the indoor environment more comfortable for high comfort occupants, when the price of electricity reduces, while equation (35.c) maintains the indoor temperature at the reference temperature set-point. The new set-point temperature T_{sp}^t the range is given as

$$T_{z,min} \leq T_{sp}^t \leq T_{z,max} \quad (36)$$

Equation (36) suggests that the new set-point temperature T_{sp}^t should be between the minimum and maximum temperature limits of the zone set by the occupants. The T_{sp}^t constraint ensures that the thermal comfort remains within the ASHARE comfort standard for a trade-off between comfort and energy saving.

4.3 Linear Regression based HVAC Load Prediction Model

As the objective is to minimize the aggregated HVAC consumption during off-peak and peak times, while maintaining various zones' temperature close to the reference temperature set-point, for optimal scheduling of the HVAC system, it is necessary to calculate the HVAC electricity consumption as a function of the thermostat set-point in a zone. The HVAC model developed in Section 2 for a multizone office building is used to calculate the electricity consumption when the indoor temperature is maintained equal to $T_{z,ref}$. Previous thermostat controllers [43, 44, 53] do not have an HVAC model and thus these controllers cannot calculate how much electricity was consumed by HVAC nor evaluate whether the load was curtailed during off-peak/peak periods compared to normal operation. However, the proposed PBDR controller uses precise HVAC modeling for an accurate DR. The mathematical modeling presented in Section 2 is used to develop the HVAC load function for the PBDR controller. Equation (28) calculates the HVAC electricity consumption as a function of the thermostat set-point in a zone. A multizone building is initially simulated with $T_{z,ref}$ and the simulation results are calculated for each time step *t*. The change in electricity consumption is then evaluated for the increase and decrease by a_z^t steps from $T_{z,ref}$. The HVAC electricity consumption changes are calculated by subtracting the electricity consumption at the modified set-point from the consumption at the reference temperature set-point for each step. The temperature change ΔT^t that subtracts the indoor temperature from the set-point temperature is denoted by ΔT^t. A linear regression model is used to predict HVAC consumption as a function of ΔT^t during each 30-minute time step as follows:

$$P_h^t = 0.07925 \Delta T^t - 0.00291 \quad [kWh/30\ minutes] \quad (37)$$

4.4 Algorithm

The developed PBDR control strategy is systemically elaborated in algorithm 1.

Algorithm 1. PBDR control strategy procedure

for every time t,

1: Take 30-minutes ahead forecast retail electricity price P_R^t
2: Take input from various zones' occupants
$P_{cq,z}^t$, $T_{z,min}$, $T_{z,max}$, $T_{z,ref}$, a_z^t
3: Compare P_R^t and $P_{cq,z}^t$ to calculate the price difference ΔP^t in the various zones using (29) at each time step *t*.
4: Evaluate the various zones' occupants' thermal comfort preferences based on the magnitude of the price difference
5: The upper and lower bounds of the price difference $\overline{U}_{t,z}$, $\underline{U}_{t,z}$ are calculated using (31) and (32) to examine the price difference range in various zones
6: Calculate the temperature change ΔT^t as a function of the price difference ΔP^t using (33)
7: The number of price differences h_z is calculated using (34) that depends on the temperature range and the set-point

interval a_z^t in various zones

8: Calculate the new thermostat set-point T_{sp}^t with a temperature change ΔT^t from the reference temperature $T_{z,ref}$ using (35.a),(35.b) and (35.c) depending on the magnitude and polarity of the price difference ΔP^t.

9: Calculate the electricity consumption as a function of temperature change ΔT^t using (37)

4.5 Additional Functionality of Proposed Controller

The designed PBDR control strategy allows the occupants to bid an electricity price within a range of a minimum $P_{R(min)}^t$ to maximum $P_{R(min)}^t$ retail price based on their preference. However, the occupant's choice of a low bidding price may affect the aggregator profit with wider implementation of the proposed controller. The aggregator uses the RTP structure to purchase electricity from the wholesale market and then sell it to consumers for profit. However, with price fluctuation, a low choice of bidding price $P_{cq,z}^t$ equal to $P_{R(min)}^t$ by multiple consumers for an extended period may exceed the aggregator's purchasing cost over a given time horizon and cause a financial loss for it. In this case, the aggregator can restrict the consumers to choose a low bidding price $P_{cq,z}^t$ greater than the threshold price ($P_{th,z}^t$) to take part in a DR program. This restriction facilitates wider implementation of the proposed controller by allowing higher payment for the aggregator to avoid loss when required. This additional functionality paves the way for wider implementation of the proposed controllers. In this study, the threshold price $P_{th,z}^t$ is calculated based on the historical average prices of RTP for a week. We consider the previous seven days 30-minutes based forecast RTP and calculate the average price. This average price is considered as a threshold price to protect the aggregator utility with wider implementation of the proposed controller.

The threshold price $P_{th,z}^t$ can be calculated as

$$\sum_{n=n1}^{n2} \sum_{t=t1}^{t2} \frac{P_{n.t}^{RTP}}{n} \quad (38)$$

where t_1, t_2 are the working hours and n_1, n_2 are the numbers of days selected to calculate the average price of electricity.

TABLE I. Architectural Features and Thermal Parameters of Building

Building Component/Parameter	**Value**	**Unit**
Orientation	South 55°, East 158°	
Zones	5	no.
Rooms	20	no.
People/room	2	no.
Floor Area	595	m^2
Roof, Wall, Window Area/room	30, 20, 5	m^2
Lighting requirement/room	1500	Watts
Occupancy/Lighting Load time	08:00-18:00	hrs.
Time index w	24	hrs
Roof Thermal Transmittance $\cup_r$	0.312	$W/m^2.C$
Wall Thermal Transmittance $\cup_w$	1.134	$W/m^2.C$
Glass Thermal Transmittance $\cup_g$	3.120	$W/m^2.C$
Shading coefficient S_c	0.72	unitless
Coefficient of Performance *COP*	4.90	unitless
Chiller Efficiency η	86	%

4.6 Experimental Setup

In this paper, a real office building of Macquarie University located at 50° south latitude in Sydney, Australia is considered. The climate zone of the above-mentioned building is warm temperate. The building's architectural features and thermal parameters are shown in Table I. Thermal parameters are taken from [42] according to the building materials of construction and the Chiller *COP* is calculated using (6).

The building envelope consists of five zones (4 exterior and 1 interior) having 20 rooms of equal area. Zones 1, 2, 3 and 4 are in the north (3 office rooms), east (4 office rooms), south (3 office rooms) and west (4 office rooms) directions respectively, while zone 5 is in the center (6 rooms) with no exterior walls as shown in Fig. 1. Zone 5 consists of four office rooms, one kitchen and a common room with a computer and printing facility. The areas of floor, roof, wall, and window are 6400, 320, 216 and 54 ft^2 respectively. In this paper, 8:00 to 18:00 hrs occupancy is assumed for people, with lighting remaining on during this time. Each office room has two persons and two computers, with a lighting requirement of 1500 watts per room. The kitchen has two ovens, a coffee maker, and a dishwasher. The common room includes appliances such as a computer, printer, etc.

The proposed DR strategy was tested for the thermal load profile of the test building. The CL requirements for the five zones were calculated using the mathematical modeling developed in Section 2, and the HVAC demand is calculated by considering the full and dynamic occupancy pattern in zones. Full occupancy implies that a certain number of occupants are utilizing the workplace at all times during occupancy hours. However, dynamic occupancy implies that occupants are not present at the working place at all times as they may move outside for lunch, a meeting or for any other activity. Thus, sensible and latent heat gains and people CL factors that depend on the number of people in a zone at one time are reduced which consequently reduces the load on the HVAC system. The HVAC demand is highest in case of full occupancy and it reduces as a zones' load is decreased by varying the people load at various time steps as shown in Fig. 5.

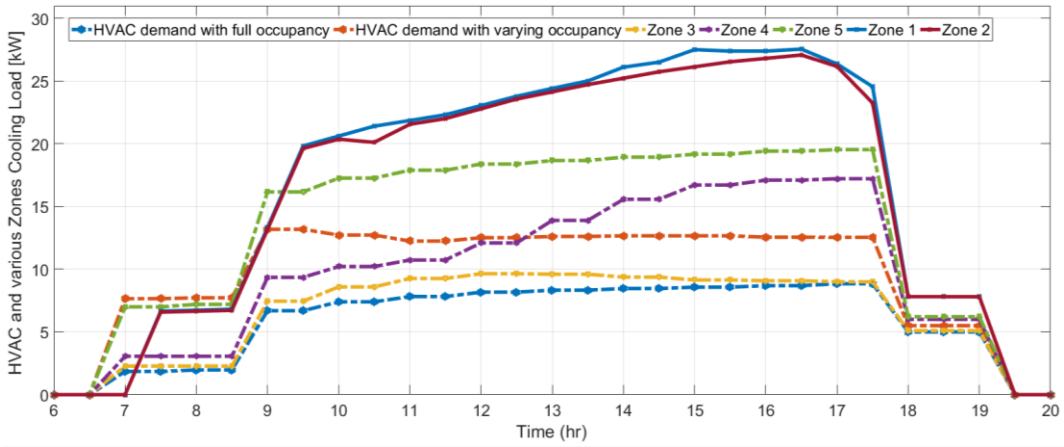

Fig. 5. Various zones' cooling load and HVAC consumption

Zones 1 to 4 face in a different direction and therefore experience variations in solar radiation at various periods. This aspect is more prominent in zone 2 and zone 4 cooling load calculation. Both zones have the same number of rooms with equal loads but different load patterns because of the varying solar radiation load factor according to the zone direction. As zone 2 is in the east direction, so solar radiation is higher than zone 4 for hrs 8 to 12 of occupancy. In contrast, the zone 4 solar load is higher than zone 2 for hrs 14 to 18 of occupancy. The cooling load in all zones increases at 8h when people start coming to work and is maintained at high levels until 18h with some fluctuations during occupancy hours. After 18h the load reduces to a low level because people leave the building.

For simulation, zones are categorized according to the occupant's thermal comfort preferences as shown in Table II.

TABLE II. Zones categorization

Zone No.	**Comfort Preferences**
Zone 1 and Zone 3	high comfort requirement
Zone 2	medium comfort requirement
Zone 4 and Zone 5	low comfort requirement

Since zone 1 and 2 have similar cooling load patterns with high comfort requirements, we assume that both zones have a similar preference in choosing a bidding price, temperature range, and set-point interval. Therefore, we only conduct simulation results for zone 1, assuming that zone 3 has similar results.

Table II demonstrates the simulation cases for the formulated building model. The conventional control represents the HVAC energy consumption at a 23ºC fixed cooling set-point temperature with a full occupancy pattern in all zones. The PBDR control strategy demonstrates the proposed algorithm results applied with a time-varying retail price. For the PBDR strategy, the experiment was performed for time-varying bidding prices, temperature ranges and set-point intervals chosen by customers in various zones according to their comfort preferences.

5. Results

In this section, simulation results are provided to evaluate the performance of the proposed PBDR controller with variable parameters. HVAC energy consumption and cost-saving results in various zones based on the bidding price are provided. Moreover, thermal comfort satisfaction based on the ASHRAE comfort standard [50] with temperature variation in various zones is evaluated.

5.1 Occupants' Bidding Prices and Thermal Preferences with High Set-Point Interval

To demonstrate the effectiveness of the proposed strategy, firstly, occupants' thermal comfort preferences in the coefficient of the bidding price and thus the temperature variation based on that bidding price are evaluated with a high set-point interval of 1ºC as shown in Figs. 6 and 7 respectively. The high set-point interval 1ºC is chosen to compare the performance with conventional control, where the thermostat setting is increased/decreased by 1ºC based on the outdoor temperature and weather conditions. Fig. 6 compares the thermal comfort preferences of occupants in various zones in the coefficient of the bidding price. It shows the 10-h profile of the 0.5-h average retail price, the bidding price and the price difference of the retail and bidding price in various zones. Figs. 6(a)(b) uncover that zone 1 and 2 occupants with high and moderate comfort preferences respectively bid a price higher than the retail price at the start of working hours (i.e., t= 8 to 9h) to maximize their comfort, and for the rest of the working hours, their bidding price is close to the retail price to maintain the desired comfort. This effect is more evident at times of low retail price (i.e., t = 9.5 – 16h) and during that time the price difference is zero in zone 1.

Meanwhile, zone 2 reasonably varies the bidding price from the retail price for a low positive price difference. However, when the electricity price significantly increases (i.e., t > 16h), zones 1 and 2 bid the maximum price (i.e., 0.18 and 0.14 $/kWh) to remain within their desired comfort zone, which is 22 to 25ºC and 22 to 26ºC respectively as shown in Figs. 7(a)(b). Even though occupants bid the maximum price at times of highest retail price, it is not very close to the retail price, which results in a noticeable price difference in both zones, and it is higher in zone 2. Likewise, Figs. 6(c)(d) show the bidding price based on the retail price in zones 4 and 5 respectively. These zones with a low comfort requirement bid quite low in response to the retail price for most of the working hours, which results in a high positive price difference. Though both of the zones have a low comfort requirement, the main difference is that the zone 5 maximum bidding price (maximum temperature limit) is lower (higher) than zone 4. This implies that at times of high retail price zone 5 occupants have high a positive price difference compared to zone 4 (i.e., t 16 to 18 h). Overall, different zones' bidding price comparison reveals that as occupants' comfort requirement reduces they more frequently and vary the bid price considerably from the retail price, which results in a high positive price difference, specifically at times of a high retail price.

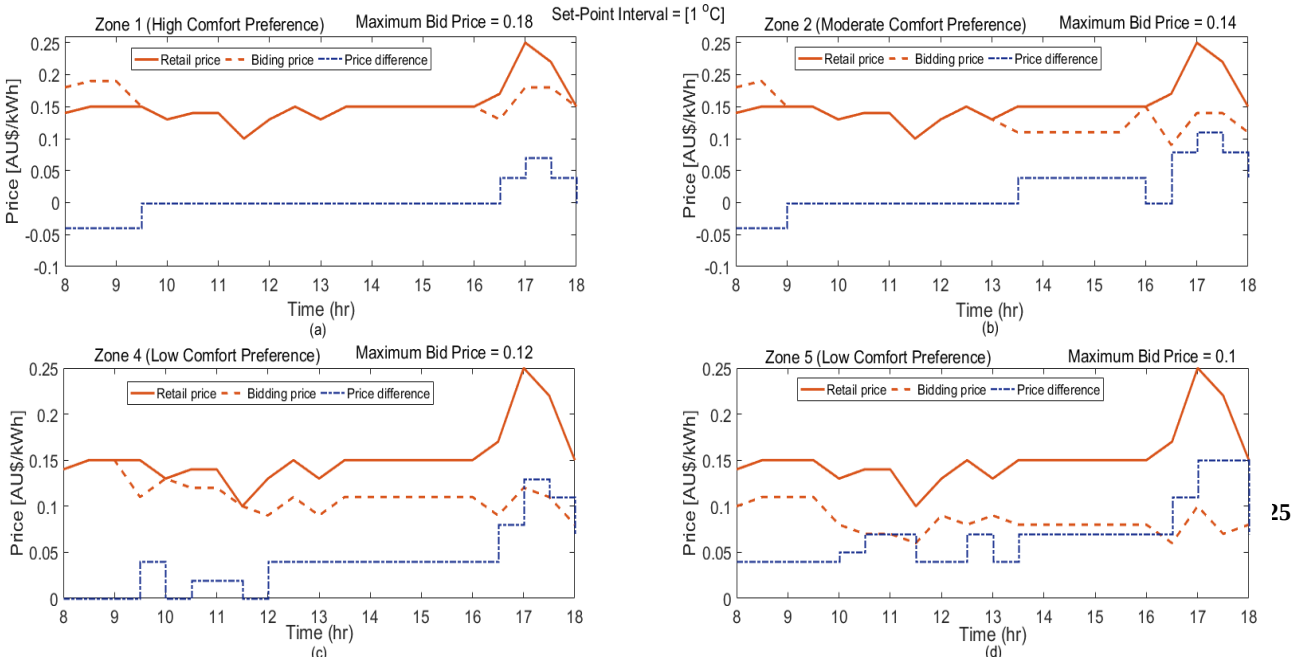

Fig. 6. Bidding Price and price difference in various zones at a set-point interval of 1ºC

Fig. 7 compares the temperature variation in various zones in response to price differences as shown in Fig. 6. It shows the 10-h profile of the 0.5-h average retail price and temperature variation in various zones. The temperature variation is the temperature difference between the reference temperature and the modified temperature in response to the bidding price. For example, a 3ºC variation means that the modified temperature is 3ºC higher than the reference temperature. However, the temperature does not abruptly vary from the reference temperature in the one-time step because of the set-point interval of 1ºC chosen by the occupants of all zones. The set-point interval of 1ºC indicates that at each time step the temperature variation from the previous set-point is limited to 1ºC. Figs. 7(a)(b) reveal that in zones 1 and 2 the thermostat set-point is reduced from the reference temperature by -1ºC for t= 8 to 9h and the modified set-point is calculated using (35.b). This is because, in these zones for the mentioned price, occupants' bidding price is higher than the retail price as shown in Figs. 6(a)(b), which results in a negative price difference using (30), and consequently the temperature is reduced. These occupants prefer to decrease the cooling set-point at the start of the working hours to maintain the thermal zone at a comfortable level for the time ahead when the temperature may increase considerably in response to a high retail price. In zones 1 and 2, the temperature variation is 0 to 1ºC at times of low retail price, however, it increases up to 2 and 3ºC respectively based on the price difference when the retail price significantly increases (i.e., t= 17h). In zones 4 and 5, based on the price difference, the zone temperature fluctuates throughout the period, however, temperature variations are more frequent and higher in zone 5 because of the high positive price difference compared to zone 4 as shown in Figs. 7(c)(d). This suggests that zone 5 occupants' maximum temperature limit is higher than in zone 4 for time steps when the retail price climbs for a trade-off between comfort and cost-saving.

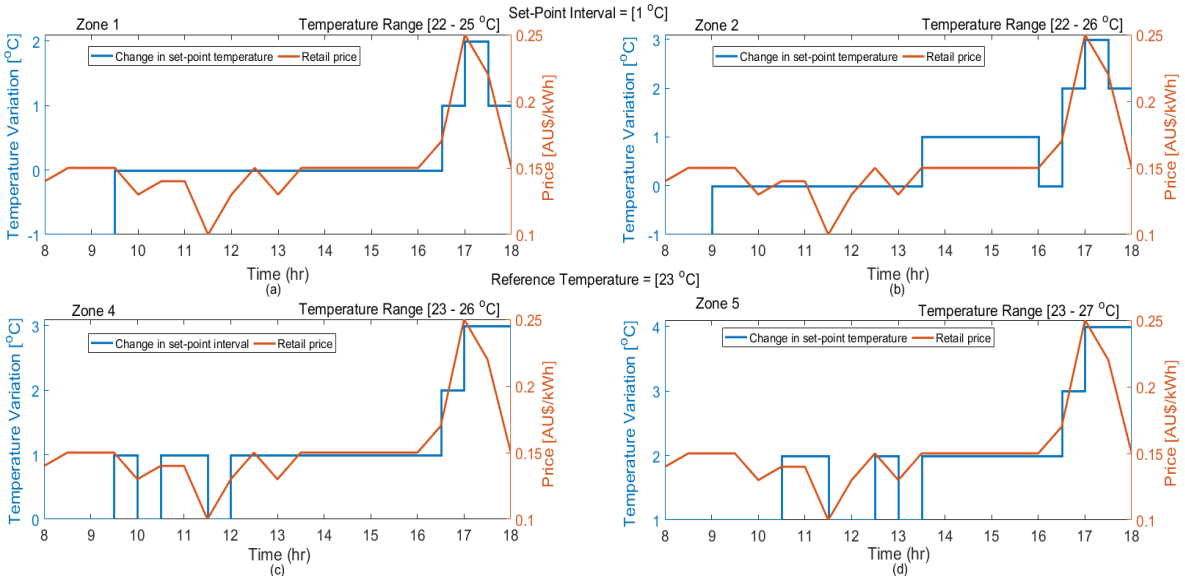

Fig. 7. Temperature variation in various zones as a function of bidding price at a set-point interval of 1ºC

5.2 Occupants' Bidding Prices and Thermal Preferences with Lower Set-Point Interval

Here, the simulation results are obtained with similar parameter settings as in the previous case but with the low set-point interval of 0.25ºC. These results provide insight into the set-point interval's effect on the bidding price and consequently the temperature variation in various zones. Fig. 8, in comparison with Fig. 7, reveals that the temperature changes more frequently in various zones with a set-point interval of 0.25ºC during simulation hours. This is because the occupants in various zones do not prefer high-temperature changes for energy saving in response to the retail price, therefore they prefer to maintain a constant thermostat setting until the price remains within a certain limit as shown in Fig. 8. However, with a low set-point interval the occupants have an opportunity to change their comfort preferences following the retail price with low-temperature changes that have a minimal impact on human comfort. The high and low

set-point interval effect on the bidding price and thus on temperature variations is more evident in zone 1, which has a high comfort preference as shown in Figs. 6(a) and 8(a). That comparison reveals that in zone 1 the bidding price is higher with a set-point interval of 1°C than with 0.25°C (i.e., t = 9 to 16h) to avoid high-temperature changes from the reference set-point. A similar effect can be observed in other zones, for instance, in zone 5 for t= 13.5 to 16.5h the thermostat setting remains constant with a set-point interval of 1°C, however, it constantly changes with a 0.25°C set-point interval for the same time. The results shown in Figs. 8(c)(d) indicates that the design algorithm overcomes the group level presentation of an occupant's thermal comfort in a multizone building and changes the thermostat setting in various zones in the coefficient of the bidding price. Also, the proposed strategy takes into account the preferred set-point interval of the occupants in each zone to cater to the varying preferences about temperature changes.

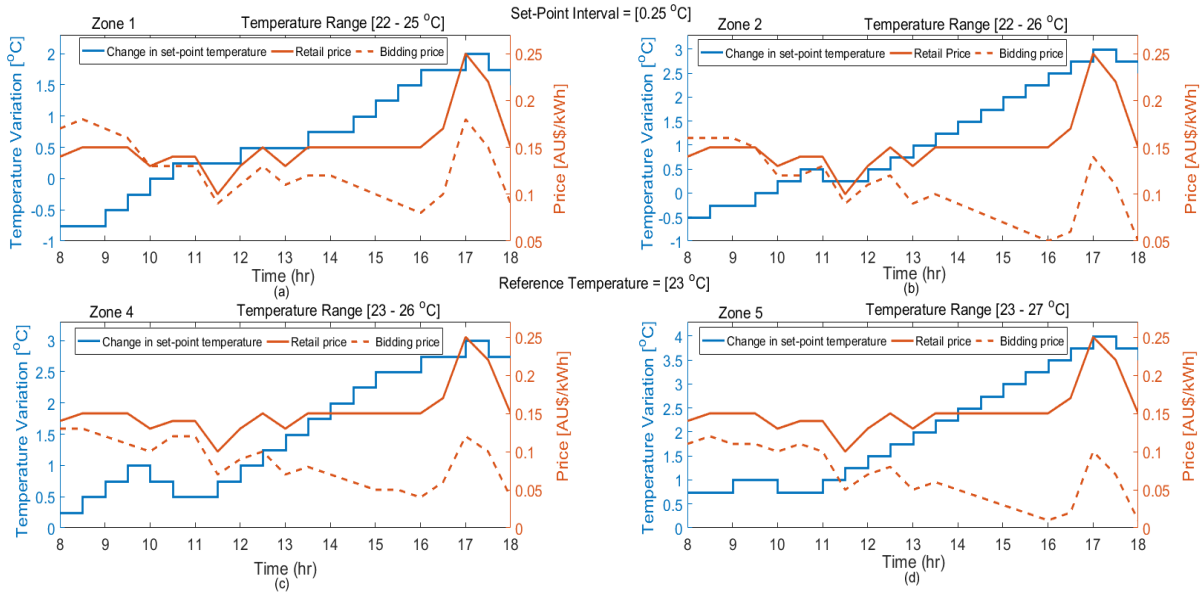

Fig. 8. Bidding price and temperature variation in various zones at a set-point interval of 0.25°C

5.3 Comparison of Bidding Price and Price Difference in two Zones at various Set-Point intervals

In this part, the relationship between the total bidding price, the price difference, and the set-point interval is examined. The occupants' total bidding price and the price difference during the simulation hours at various set-point intervals are calculated in two chosen zones. Zones 1 and 5 are selected because they represent two extremes, high and low comfort preference zones respectively. Fig. 9 compares the aggregated bidding price and the price difference in zones 1 and 5 at three different set-point intervals 0.25, 0.5 and 1°C, and further, it shows a comparison between the aggregated electricity cost with conventional control and bidding price. The results reported here indicate that the occupants' aggregated bidding price is positively correlated with the set-point interval, and it is significantly higher in high comfort zones compared to low comfort zones. For instance, the aggregated bidding price increases from 2.65 to 3.17 and 1.42 to 1.76 AU$/kWh in zones 1 and 5 respectively, with changes in the set-point interval from 0.25 to 1°C. This shows a 16.4 and 19.1% reduction in electricity cost per kWh with changes in the set-point interval from 1 to 0.25°C for zones 1 and 5 respectively. From these results, it can be further inferred that, with the proposed strategy, high and low comfort occupants can save 0.94 to 17.1% and 45.0 to 55.6% on the electricity cost per kWh with set-point intervals of 1 to 0.25°C respectively compared to conventional control. On the other hand, the price difference is negatively correlated with the set-point interval because a higher bidding price in a zone leads to a lower positive price difference. For instance, the price difference in zone 5 decreases from 1.78 to 1.69 AU$/kWh with a change in the set-point interval from 0.25 to 0.5°C.

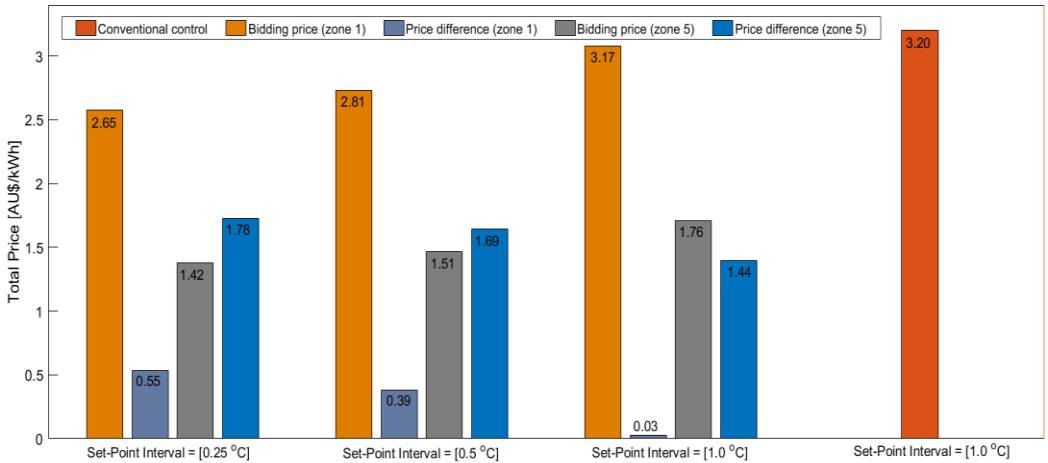

Fig. 9. Aggregated bidding price and price difference at various set-point intervals

5.4 Effect of Various Set-Point Intervals on HVAC Consumption in various Zones

Fig. 10 shows the effect of temperature variations in various zones on the HVAC energy consumption evaluated at two set-point intervals, and further compares the HVAC demand with conventional and PBDR control strategies. In conventional control, the HVAC is operated to maintain a reference temperature (23°C) in a multizone building for t= 8 to 18h regardless of the retail price. In contrast, the PBDR control strategy causes a regular change in the HVAC thermostat setting in various zones based on the electricity price. The simulation results show that the HVAC load in various zones is curtailed compared to conventional control, with temperature variations for energy and cost-saving. The HVAC demand at a constant reference temperature and variable temperature set-points are subtracted for $8\text{h} \leq t \leq 18\text{h}$ to calculate the energy saving in various zones. It is clear from Fig. 10 that the HVAC demand with conventional control is higher in all zones than the PBDR control strategy except for t= 8 to 9h in zones 1 and 2, where the occupants bid higher than the retail price to decrease the cooling set-point from the reference temperature. The case study results reveal that at both set-point intervals the energy consumption in low comfort zones (i.e., zones 4 and 5) is significantly lower than in the moderate and high comfort zones following high-temperature variations in these zones. However, at a lower set-point interval the HVAC operation constantly changes and causes an additional reduction in HVAC consumption, specifically in peak hours (i.e., $15\text{h} \leq t \leq 17.5\text{h}$) compared to the case with a higher set-point interval. This indicates that with similar parameter settings the designed controller with a low set-point interval causes more reduction in HVAC demand than with a higher set-point interval.

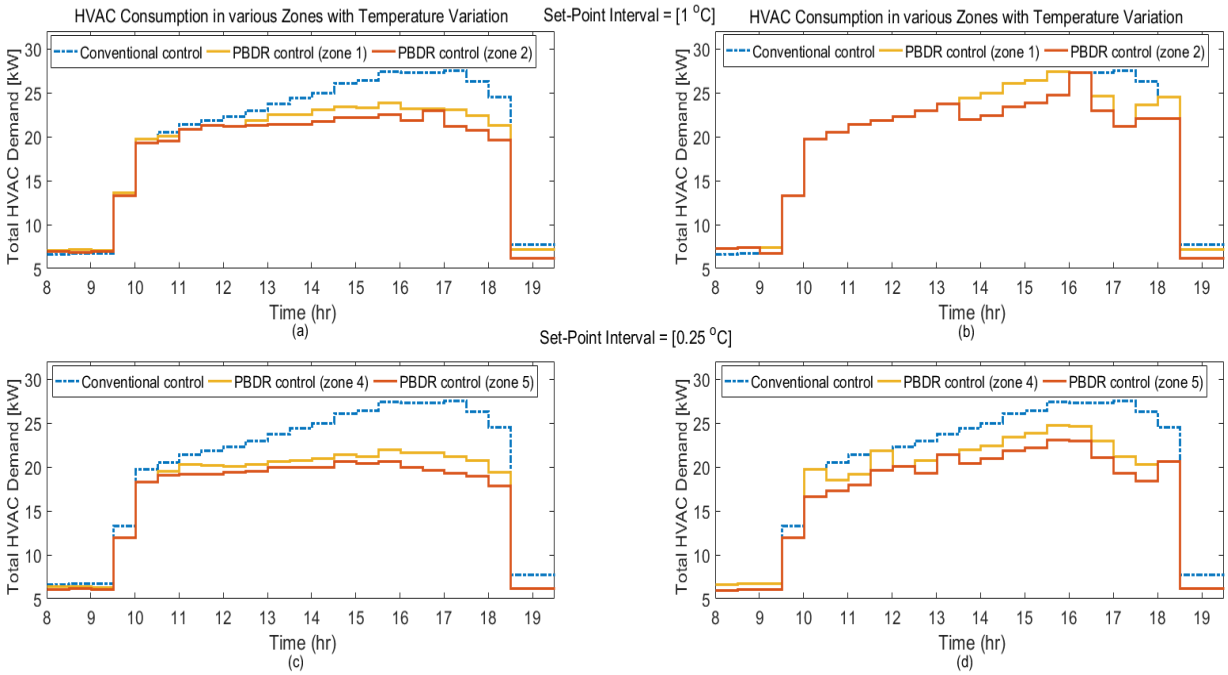

Fig. 10. Significant reduction in HVAC energy consumption with PBDR controller in various zones at two set-point intervals

5.5 Comparison of HVAC Energy and Cost Saving in various Zones

Table III provides a comparison of the percentage of HVAC energy and cost savings under conventional and PBDR control. The saving results at a higher set-point interval with the PBDR strategy is compared with conventional control; further, the higher and lower set-point interval results with the PBDR controller are evaluated. The proposed controller allocates the variable temperature set-points in various zones for each half-hour of the day that is used as thermostat set-points to control the HVAC load with the retail price. The results reported in Table III suggest that the designed algorithm

operates effectively to reduce the aggregated peak demand, off-peak demand and electricity cost during off-peak and peak times, considering the comfort requirement of various types of occupants. For instance, zone 1 occupants with high comfort requirements can reduce the HVAC demand by 2.15 and 7.19% during off-peak and peak times respectively, compared to conventional control with a set-point interval of 1ºC. This energy-saving corresponds to 3.36 and 8.90% curtailments in electricity cost with indoor temperature variations for only a tiny fraction of the given time. These occupants' energy and cost-saving are 14.34 and 14.55% respectively during peak times with a 0.25ºC set-point interval that is 43.0% higher than for a 1ºC set-point interval. These saving results indicate that the proposed strategy with low-temperature changes is very effective to save energy and cost with minimal effect on human health. It is clear from Table III that the aggregated demand of the HVAC system is significantly lower with the proposed strategy than with conventional control. For example, the aggregated demand with conventional control is 449.04 kWh during occupancy hours that is reduced to 412.8 and 362.9 kWh in high to low comfort zones (i.e., zones 1 and 5) respectively with the designed controller operating at high set-point intervals. This corresponds to 8.06 to 19.17% curtailments in the HVAC demand during the simulation hours compared to conventional control. Similarly, peak saving results are achieved in various zones with the developed strategy. For instance, the peak demand reduces from 162.66 kWh to 139.33, 131.74, 128.49 and 118.99 kWh in zones 1, 2, 4 and 5 respectively with a 0.25ºC set-point interval, corresponding to 14.55, 19.45, 21.21 and 27.24% reductions in the electricity bill compared to conventional control. These results indicate that the PBDR the controller is very effective in reducing the electricity cost, specifically during peak hours when the energy price is higher.

5.6 Thermal Comfort

The proposed PBDR controller, along with energy and cost savings, can potentially introduce thermal discomfort due to constant change of the thermostat set-points in various zones based on the retail price. Thus, it is essential to evaluate the performance of the proposed strategy with respect to acceptable thermal environmental conditions for human occupancy. For this ASHRAE standard 55 [75], that establishes the range of indoor environmental conditions to achieve acceptable thermal comfort for occupants, is followed. As per the ASHRAE standard, to maintain thermal comfort the humidity ratio should be ≤ 12 moisture/kilogram of dry air and the dew point temperature < 18 ºC. Fig. 11 shows the comfort zone of the test building in summer drawn on a psychometric chart with a metabolic rate of 1.2 met and clothing insolation of 0.6 clo according to the considered building working environment. The green line indicates the upper limit of the dew point temperature, while the orange line represents the maximum allowable humidity ratio. The comfort zone shows the indoor temperature variation in various zones in response to the retail price. Fig. 11 results indicate that the indoor temperature variations are within the comfort zone. This implies that under PBDR control occupants can enjoy significant cost saving with temperature variations in various zones within the ASHRAE comfort zone.

TABLE III. Comparison of Aggregated Daily Energy and Cost Saving for Base Case and Case 1

HVAC Control	**Zone**	**Temp Range**	**Set-Point Interval**	**HVAC Demand Off-Peak Hours**	**HVAC Demand Peak Hours**	**Energy Cost Off-Peak Hours**	**Energy Cost Peak Hours**	**Energy Saving Off-Peak Hours**	**Energy Saving Peak Hours**	**Cost Saving Off-Peak Hours**	**Cost Saving Peak Hours**
	No.	**ºC**	**ºC**	**kWh**	**kWh**	**AU$**	**AU$**	**%**	**%**	**%**	**%**
Conventional		23	1.0	449.04	162.66	69.61	29.55	---	---	---	---
PBDR Controller	Zone 1	22-25	1.0	439.35	150.95	67.27	26.92	2.15	7.19	3.36	8.90
			0.25	412.8	139.33	63.45	25.25	8.06	14.34	8.84	14.55
	Zone 2	22-26	1.0	417.30	139.59	63.82	25.07	7.06	14.18	8.31	15.16
			0.25	395.92	131.74	60.65	23.80	11.80	19.09	12.87	19.45
	Zone 4	23-26	1.0	400.20	137.74	61.27	24.66	10.87	15.32	11.98	16.54
			0.25	381.7	128.49	58.61	23.28	14.98	21.07	15.80	21.21
	Zone 5	23-27	1.0	373.82	127.17	57.2	22.72	16.75	21.81	17.82	23.11
			0.25	362.9	118.99	55.49	21.50	19.17	26.84	20.27	27.24

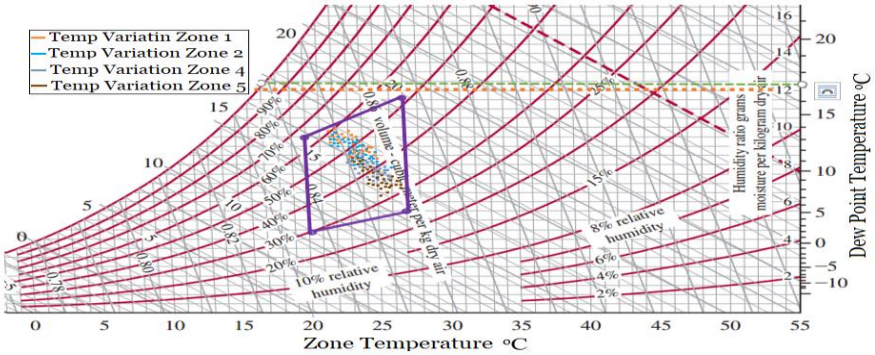

Fig. 11. Comfort zone for a commercial building in the summer season

Fig. 12 provides the percentage of time when the zone temperature is more than the reference temperature at two set-point intervals for the simulation hours. The case study results report that, for customers with high comfort preferences, the indoor temperature stays at 23 ºC for 71.4% of the occupancy hours. For these customers, temperature excursions of -1, +1 and +2 ºC from the reference temperature (23 ºC) occur in 14.2, 9.50 and 4.76% of the occupied hours respectively with a set-point interval of 1ºC. Similarly, in zones 4 and 5, +2 and +3ºC excursions occur around 57.4 and 52.38% of the occupied time respectively. Meanwhile, zone 2, with a moderate comfort requirement, is +1 and +2 ºC away from the reference temperature for 33.3% and 9.50% of the occupancy hours respectively. Similar temperature variation patterns with more fluctuations occur at a set-point interval of 0.25 ºC. For instance, occupants with a low comfort requirement in zone 5 maintain the thermostat setting between 23-24ºC and 24-25ºC for 28.57% and 19.05% of the occupancy time, while a 4ºC excursion occurs only for 4.76% of the occupied hours. It should be noted that the customer preferences for the comfort required are stringently maintained by the proposed strategy. The thermal comfort, therefore, is not overly disturbed through the implementation of the proposed PBDR strategy.

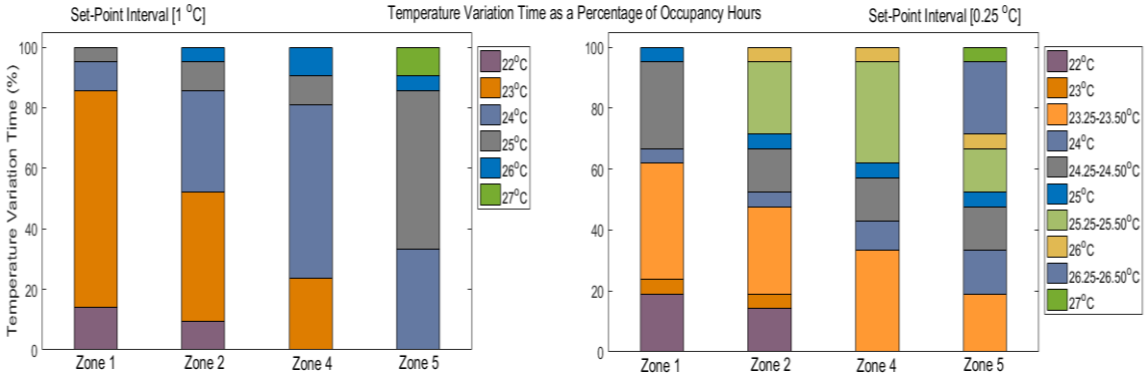

Fig. 12. Percentage of time when the indoor temperature is below/above the reference temperature

6. Discussion

In this section, the findings are discussed in comparison with related literature to signify the importance of the proposed approach over existing approaches for implementation. The following are the main contributions in comparison with the latest most relevant published works [43, 51].

- The work in [51] uses the ratio of weighted coefficients for occupants' thermal discomfort and the average price of electricity to trigger HVAC set-point temperature change in comparison to the current electricity price at time *t*. However, using this ratio as a trigger is not suitable for high variations of electricity prices in the real-time market. This may cause the controller to not increase the thermostat setting when the load should be curtailed. As a result, electricity consumers may not have benefits to save electricity costs by reducing their consumption during peak periods. The electricity cost saving of an HVAC unit with a high thermal discomfort level using a price-based strategy in [40] is 17.3%. Unlike, the proposed controller uses the price difference between the current retail price and the dynamic bidding price that occupants change at each time step in various zones. This way the proposed strategy can control the HVAC thermostat setting considering fluctuations in electricity retail prices for more saving of energy cost than the controller in [40]. Using the proposed controller, the electricity cost saving with high thermal discomfort during peak and off-peak hours are 27.2 and 20.3% respectively as shown in Table III. This result demonstrates a further reduction in energy use at a high priced period than the controller developed in [40].
- In respect to energy consumption in [51], the variable speed heat pumps were schedules to operate with high power inputs during the hours when occupants' thermal discomfort level is high which results in high energy

consumption. The occupant's thermal discomfort can be high in the hours when the peak demand occurs during the high price period, thus in this case, the developed strategy may not be able to cut peak electricity consumption if implemented by electric utility companies. The simulation results provided in [40] does not show how much energy can be saved during peak hours by implementing the developed approach. Contrasting, the numerical results of this paper reported in Table III demonstrate that the proposed strategy is effective to reduce the peak load varies from 7.19 to 26.8% contingent on occupant's thermal preferences, and thus enable the utility providers to adopt effective demand management using real-time pricing.

- In [51] the minimum and maximum temperature limit which is determined by the standards for building space conditions, and the temperature change rate in each zone (controlled by building operators) is constant and the same (1^{o}C). Unlike [51], in the proposed work, the occupants can select variable temperature limits within a specified building occupancy standards in each zone. Moreover, the occupants can vary the temperature change rate in each zone from (0.25 to 1^{o}C) based on their preference. The simulation result demonstrates that the HVAC consumption is minimum at low-temperature change rate compared to the high-temperature change rate in each zone as depicted in Table III. Moreover, the low-temperature change rate has minimal impacts on human health by reducing thermal shock and also reduces the mechanical burden to the heat pump. The temperature change rate effect is not taken into account in [40], thus the proposed method is more advantageous, practical and dynamic.

7. Conclusion

In this paper, an easily deployable and improved PBDR control strategy in a real-time environment was is proposed to control a multi-zone office building HVAC load while considering the varying thermal comfort preferences of occupants. An ANN was employed to model the occupants varying thermal comfort preferences as a coefficient of bidding price. Dynamic HVAC thermostat setting in each zone was determined by developing a control mechanism based on the ANN prediction model results. The numerical results indicate that the proposed technique brings significant peak load curtailments of 7.19 to 21.7% and 14.34 to 26.84% for high to low comfort occupants at 1 and 0.25^{o}C set-point intervals respectively. This implies an 8.91 to 21.21% and 14.55 to 27.24% saving on a peak electricity bill correspondingly. Moreover, the indoor air temperature is mostly maintained inside the thermal comfort zone. For customers with lower comfort preferences of about 4.76% to 9.50% of the total hours of occupancy, the temperature becomes +3 and +4 ^{o}C higher than the reference temperature. This implies that, when the thermostat is varied during periods of high electricity price, the developed strategy does not cause a noteworthy change in the thermal discomfort. The obtained results through extensive simulation studies under various conditions demonstrate the effectiveness and applicability of the proposed strategy.

In contrast to existing strategies, where a group level presentation of occupants' thermal comfort, high-temperature change rate and fewer user control were implemented in a multizone building, the developed PBDR controller successfully reflects the varying thermal preferences of the occupants for optimal scheduling of the HVAC operation. For utilities and RESs integrated building operators, a real-time wholesale price based tariff is effective to reduce the peak load, the overall electricity consumption, and energy imbalance management. This may assist utilities in avoiding the cost of constructing additional power plants and transmission lines, with associated maintenance. The PBDR control procedure allows consumers to successfully take advantage of dynamic pricing and enjoy substantial cost savings in electricity usage. Alternatively, this plan can contribute greatly in facilitating an effective DR framework, enabling the utility provider to adopt effective demand management policies using RTP. Based on the achievements in this paper, an interesting extension of this work is to increase the scalability of the proposed approach by including a higher number of HAC units. Moreover, the load recovery effect, which generally appears after limiting the power of HVACs during a DR event period, can be examined for a fairer comparison with existing techniques. Another direction could be recording the number of occupants in real-time for instantaneous load calculation if a large number of occupants shared one room/commonplace while considering the dynamic comfort preferences in a zone.

References

[1] Australian Sustainable Built Environment Council (ASBEC), "The Second Plank: Building a Low Carbon Economy with Energy Efficient Buildings," The University of Melbourne Energy Research Institute, 2008.

[2] "Commercial Building Disclosure: A National Energy Efficiency Program", Australian Government Department of the Environment and Energy, 2011.

[3] "Country Energy's Electricity Network Revised Regulatory Proposal 2009-2014", Essential Energy, 16 January 2009.

[4] "Guide to Best Practice Maintenance & Operation of HVAC Systems for Energy Efficiency", Council of Australian Governments (COAG) National Strategy on Energy Efficiency, January 2012.

[5] J. Claridge, "Innovative HVAC Program Report: Demand Management and Planning Project", NSW Department of Planning, TransGrid and Energy Australia2006.

[6] "Ausgrid, Supply, and Demand: our five-year network plan", 2011-12.

[7] "ENA Submission to Senate Committee Inquiry on Electricity Prices", Energy Network Association 2012.
[8] W. Chiu, H. Sun, and H. V. Poor, "Energy Imbalance Management Using a Robust Pricing Scheme," *IEEE Transactions on Smart Grid*, vol. 4, pp. 896-904, 2013.
[9] S. Bahrami, Y. C. Chen, and V. W. S. Wong, "An Autonomous Demand Response Algorithm based on Online Convex Optimization", in *2018 IEEE International Conference on Communications, Control, and Computing Technologies for Smart Grids (SmartGridComm)*, 2018, pp. 1-7.
[10] S. Bahrami, M. H. Amini, M. Shafie-khah, and J. P. S. Catalão, "A Decentralized Electricity Market Scheme Enabling Demand Response Deployment," *IEEE Transactions on Power Systems*, vol. 33, pp. 4218-4227, 2018.
[11] "Benefits of demand response in electricity markets and recommendations for achieving them," U.S. Department of Energy, February 2006.
[12] "Assessment of Demand Response and Advanced Metering," Federal Energy Regulatory Commission November 2018.
[13] R. Deng, Z. Yang, M. Chow, and J. Chen, "A Survey on Demand Response in Smart Grids: Mathematical Models and Approaches," *IEEE Transactions on Industrial Informatics*, vol. 11, pp. 570-582, 2015.
[14] M. Chertkov and V. Chernyak, "Ensemble of Thermostatically Controlled Loads: Statistical Physics Approach," *Scientific Reports*, vol. 7, p. 8673, 2017.
[15] J. Shen, C. Jiang, and B. Li, "Controllable Load Management Approaches in Smart Grids," *Energies*, vol. 8, pp. 11187-11202, 2015.
[16] H. Hao, C. D. Corbin, K. Kalsi, and R. G. Pratt, "Transactive Control of Commercial Buildings for Demand Response," *IEEE Transactions on Power Systems*, vol. 32, pp. 774-783, 2017.
[17] K. Zhang, Y. Mao, S. Leng, S. Maharjan, Y. Zhang, A. Vinel, *et al.*, "Incentive-Driven Energy Trading in the Smart Grid," *IEEE Access*, vol. 4, pp. 1243-1257, 2016.
[18] R. A. D.hammerstrom, J.Brous, "Pacific Northwest Gridwise Testbed Demonstration Projects," Pacific Northwest Nat. Lab., Rich-land, WA, USA 2007.
[19] K. S. S.E.Widergren, J.C. Fuller, "AEP Ohio grid smart demonstration project real-time pricing demonstration analysis," Pacific NorthwestNat.Lab., Richland, WA, USA, Tech.Rep.PNNL-23192, 2014.
[20] E. Fernandez, P. Jamborsalamati, M. J. Hossain, and U. Amin, "A communication-enhanced price-based control scheme for HVAC systems," in *2017 IEEE Innovative Smart Grid Technologies - Asia (ISGT-Asia)*, 2017, pp. 1-6.
[21] D. P. C. S.Katipamula, D.D.Hatley, "Transactive Controls: Market-Based Gridwise Controls for Building System," Pacific Northwest Nat. Lab., Rich-land, WA, USA 2006.
[22] S. Katipamula, "Transactive Controls in Buildings: Challenges and Opportunities," *DOE Electricity Advisory Committee Meeting*, 2016.
[23] F. Rahimi, A. Ipakachi, and F. Fletcher, "The Changing Electrical Landscape: End-to-End Power System Operation under the Transactive Energy Paradigm," *IEEE Power and Energy Magazine*, vol. 14, pp. 52-56, 2016.
[24] K. X. Perez, M. Baldea, and T. F. Edgar, "Integrated smart appliance scheduling and HVAC control for peak residential load management," in *2016 American Control Conference (ACC)*, 2016, pp. 1458-1463.
[25] D. T. Vedullapalli, R. Hadidi, and B. Schroeder, "Optimal Demand Response in a building by Battery and HVAC scheduling using Model Predictive Control," in *2019 IEEE/IAS 55th Industrial and Commercial Power Systems Technical Conference (I&CPS)*, 2019, pp. 1-6.
[26] C. Petrie, S. Gupta, V. Rao, and B. Nutter, "Energy-Efficient Control Methods of HVAC Systems for Smart Campus," in *2018 IEEE Green Technologies Conference (GreenTech)*, 2018, pp. 133-136.
[27] A. Tyukov, M. Shcherbakov, A. Sokolov, A. Brebels, and M. Al-Gunaid, "Supervisory model predictive on/off control of HVAC systems," in *2017 8th International Conference on Information, Intelligence, Systems & Applications (IISA)*, 2017, pp. 1-7.
[28] Y. Li, J. D. L. Ree, and Y. Gong, "The Smart Thermostat of HVAC Systems Based on PMV-PPD Model for Energy Efficiency and Demand Response," in *2018 2nd IEEE Conference on Energy Internet and Energy System Integration (EI2)*, 2018, pp. 1-6.
[29] S. Mohajeryami, I. N. Moghaddam, M. Doostan, B. Vatani, and P. Schwarz, "A novel economic model for price-based demand response," *Electric Power Systems Research*, vol. 135, pp. 1-9, 2016.
[30] M. Tavakkoli, S. Fattaheian-dehkordi, M. Pourakbari-kasmaei, M. Liski, and M. Lehtonen, "An Incentive-Based Demand Response by HVAC Systems in Residential Houses," in *2019 IEEE PES Innovative Smart Grid Technologies Europe (ISGT-Europe)*, 2019, pp. 1-5.
[31] H. J. Monfared, A. Ghasemi, A. Loni, and M. Marzband, "A hybrid price-based demand response program for the residential micro-grid," *Energy*, vol. 185, pp. 274-285, 2019.
[32] J. Cao, B. Yang, K. Ma, C. Chen, and X. Guan, "Residential HVAC load control strategy based on game theory," in *2017 Chinese Automation Congress (CAC)*, 2017, pp. 5933-5938.
[33] J. H. Yoon, R. Baldick, and A. Novoselac, "Dynamic Demand Response Controller Based on Real-Time Retail Price for Residential Buildings," *IEEE Transactions on Smart Grid*, vol. 5, pp. 121-129, 2014.
[34] M. Alhaider and F. Lingling, "Mixed-integer programming for HVACs operation," in *2015 IEEE Power & Energy Society General Meeting*, 2015, pp. 1-5.

[35] O. Erdinc, A. Tascikaraoglu, N. G. Paterakis, Y. Eren, and J. Catalao, "End-user comfort-oriented day-ahead planning for responsive residential HVAC demand aggregation considering weather forecasts," in *2017 IEEE Power & Energy Society General Meeting*, 2017, pp. 1-1.
[36] S. k. Gupta, T. Ghose, and K. Chatterjee, "Droop Based Dynamic Demand Response Controller for HVAC Load," in *2018 20th National Power Systems Conference (NPSC)*, 2018, pp. 1-6.
[37] G. S. Pavlak, G. P. Henze, and V. J. Cushing, "Optimizing commercial building participation in energy and ancillary service markets," *Energy and Buildings*, vol. 81, pp. 115-126, 2014.
[38] E. M. Greensfelder, G. P. Henze, and C. Felsmann, "An investigation of optimal control of passive building thermal storage with real-time pricing," *Journal of Building Performance Simulation*, vol. 4, pp. 91-104, 2011.
[39] S. Bhattacharya, K. Kar, and J. H. Chow, "Economic Operation of Thermostatic Loads under Time-Varying Prices: An Optimal Control Approach," *IEEE Transactions on Sustainable Energy*, pp. 1-1, 2018.
[40] A. Abdulaal and S. Asfour, "A linear optimization-based controller method for real-time load shifting in industrial and commercial buildings," *Energy and Buildings*, vol. 110, pp. 269-283, 2016.
[41] G. Goddard, J. Klose, and S. Backhaus, "Model Development and Identification for Fast Demand Response in Commercial HVAC Systems," *IEEE Transactions on Smart Grid*, vol. 5, pp. 2084-2092, 2014.
[42] D. Christantoni, S. Oxizidis, D. Flynn, and D. P. Finn, "Implementation of demand response strategies in a multi-purpose commercial building using a whole-building simulation model approach," *Energy and Buildings*, vol. 131, pp. 76-86, 2016.
[43] E. Biyik, S. Genc, and J. D. Brooks, "Model predictive building thermostatic controls of small-to-medium commercial buildings for optimal peak load reduction incorporating dynamic human comfort models: Algorithm and implementation," in *2014 IEEE Conference on Control Applications (CCA)*, 2014, pp. 2009-2015.
[44] L. Ciabattoni, G. Cimini, F. Ferracuti, M. Grisostomi, G. Ippoliti, and M. Pirro, "Indoor thermal comfort control through fuzzy logic PMV optimization," in *2015 International Joint Conference on Neural Networks (IJCNN)*, 2015, pp. 1-6.
[45] M. Nowak and A. Urbaniak, "Utilization of intelligent control algorithms for thermal comfort optimization and energy-saving," in *2011 12th International Carpathian Control Conference (ICCC)*, 2011, pp. 270-274.
[46] Y. Pang, G. Hu, and C. J. Spanos, "Distributed Model Predictive Control of an HVAC System via a Projected Subgradient Method," in *2018 IEEE 14th International Conference on Control and Automation (ICCA)*, 2018, pp. 878-883.
[47] A. Yasuoka, H. Kubo, K. Tsuzuki, and N. Isoda, "Gender Differences in Thermal Comfort and Responses to Skin Cooling by Air Conditioners in the Japanese Summer," *Journal of the Human-Environment System*, vol. 18(1):011-020, October 2015.
[48] Z. Gou, W. Gamage, S. Siu-Yu Lau, and S. Sing-Yeung Lau, "An investigation of thermal comfort and adaptive behaviors in naturally ventilated residential buildings in tropical climates: a pilot study," *Buildings*, vol. 8, 3 January 2018.
[49] V. L. Erickson and A. E. Cerpa, "Thermovote: Participatory Sensing for Efficient Building HVAC Conditioning," presented at the Proceedings of the Fourth ACM Workshop on Embedded Sensing Systems for Energy-Efficiency in Buildings, Toronto, Canada, 2012.
[50] A. Ghahramani, F. Jazizadeh, and B. Becerik-Gerber, "A knowledge-based approach for selecting energy-aware and comfort-driven HVAC temperature set points," *Energy and Buildings*, vol. 85, pp. 536-548, 2014.
[51] Y. Kim, "Optimal Price Based Demand Response of HVAC Systems in Multizone Office Buildings Considering Thermal Preferences of Individual Occupants Buildings," *IEEE Transactions on Industrial Informatics*, vol. 14, pp. 5060-5073, 2018.
[52] M. Elnour and N. Meskin, "Multi-zone HVAC control system design using feedback linearization," in *2017 5th International Conference on Control, Instrumentation, and Automation (ICCIA)*, 2017, pp. 249-254.
[53] P. M. Ferreira, A. E. Ruano, S. Silva, and E. Z. E. Conceição, "Neural networks based predictive control for thermal comfort and energy savings in public buildings," *Energy and Buildings*, vol. 55, pp. 238-251, 2012.
[54] R. Z. Homod, "Review on the HVAC System Modeling Types and the Shortcomings of Their Application," *Journal of Energy* vol. 2013, Article ID 768632, p. 10, 2013.
[55] X. Lü, "Modelling of heat and moisture transfer in buildings: I. Model program," *Energy and Buildings*, vol. 34, pp. 1033-1043, 2002.
[56] S. Goyal and P. Barooah, "A method for model-reduction of non-linear thermal dynamics of multi-zone buildings," *Energy and Buildings*, vol. 47, pp. 332-340, 2012.
[57] M. Avci, M. Erkoc, A. Rahmani, and S. Asfour, "Model predictive HVAC load control in buildings using real-time electricity pricing," *Energy and Buildings*, vol. 60, pp. 199-209, 2013.
[58] Y.-S. Kim and J. Srebric, "Impact of occupancy rates on the building electricity consumption in commercial buildings," *Energy and Buildings*, vol. 138, pp. 591-600, 2017.
[59] S. Goubran, D. Qi, W. F. Saleh, and L. Wang, "Comparing methods of modeling air infiltration through building entrances and their impact on building energy simulations," *Energy and Buildings*, vol. 138, pp. 579-590, 2017.
[60] R. Yao, B. Li, and J. Liu, "A theoretical adaptive model of thermal comfort – Adaptive Predicted Mean Vote (aPMV)," *Building and Environment*, vol. 44, pp. 2089-2096, 2009.
[61] R. Mcdowall, *Fundamentals of HVAC Systems*: Elsevier, 2006.

[62] Y. Ma and F. Borrelli, "Fast stochastic predictive control for building temperature regulation," in *2012 American Control Conference (ACC)*, 2012, pp. 3075-3080.
[63] N. Nassif, S. Kajl, and R. Sabourin, "Evolutionary algorithms for multi-objective optimization in HVAC system control strategy," in *Fuzzy Information, 2004. Processing NAFIPS '04. IEEE Annual Meeting of the*, 2004, pp. 51-56 Vol.1.
[64] A. Kelman and F. Borrelli, "Bilinear Model Predictive Control of an HVAC System Using Sequential Quadratic Programming," *IFAC Proceedings Volumes*, vol. 44, pp. 9869-9874, 2011.
[65] N. Radhakrishnan, S. Yang, R. Su, and K. Poolla, "Token-based scheduling of HVAC Services in commercial buildings," in *2015 American Control Conference (ACC)*, 2015, pp. 262-269.
[66] Y.-W. Wang, W.-J. Cai, Y.-C. Soh, S.-J. Li, L. Lu, and L. Xie, "A simplified modeling of cooling coils for control and optimization of HVAC systems," *Energy Conversion and Management*, vol. 45, pp. 2915-2930, 2004.
[67] L. Lu, W. Cai, L. Xie, S. Li, and Y. C. Soh, "HVAC system optimization—in-building section," *Energy and Buildings*, vol. 37, pp. 11-22, 2005.
[68] *ASHRAE Handbook Fundamentals*, SI Edition ed.: Supported by ASHRAE Research, 2005.
[69] A. Bhatia, "Cooling Load Calculations and Principles," ed Stony Point, New York: Continuing Education and Development, Inc.
[70] *ASHRAE Handbook Fundamentals*, SI Edition ed.: Supported by ASHRAE Research, 1997.
[71] E. Fernandez, M. J. Hossain, and M. S. H. Nizami, "Game-theoretic approach to demand-side energy management for a smart neighborhood in Sydney incorporating renewable resources," *Applied Energy*, vol. 232, pp. 245-257, 2018.
[72] T. M. Christensen, A. S. Hurn, and K. A. Lindsay, "Forecasting spikes in electricity prices," *International Journal of Forecasting*, vol. 28, pp. 400-411, 2012.
[73] " ACCC, Applications for authorisation - National Electricity Code, 10 December 1997, p60.
[74] *Day-Ahead, Electricity Price & Demand* Available: https://www.aemo.com.au/Electricity/National-Electricity-Market-NEM/Data-dashboard
[75] A. A. S. 55-2010, "American Society of Heating, Refrigeration and Air Conditioning Engineers (ASHRAE), Thermal Environmental Conditions for Human Occupancy".